Bio-Design and Manufacturing (2026) 9:415–435
https://doi.org/10.1631/bdm.2500504

REVIEW

# Reversible electroporation: controllably opening the cellular doorway

Yuhao Zhou[1,2,3] · Zhihui Zhang[1,2,3] · Feng Liu[1,2,3] · Xinran Jiang[1,2,3] · Chaojuan Yang[1] · Yang Wang[1,3] · Zaizai Dong[1,3] · Lingqian Chang[1,3]

Received: 3 October 2025 / Accepted: 26 November 2025 / Published online: 1 May 2026


**Abstract**

Reversible electroporation (RE) involves applying pulsed electric fields to briefly disrupt cell membrane channels, allowing molecular transfer while preserving cell viability. Advances in RE combined with micro- and nano-devices have improved efficiency and safety in cellular analysis and engineering, holding substantial promise for biological research and precision medicine. This review summarizes progress in RE technology, spanning underlying theoretical principles, practical implementation, and emerging applications. By integrating mechanistic insights with parameter assessment, we strengthen process understanding of RE to support further optimization. To clarify RE implementation strategies, we present advances in micro- and nano-devices based on varying electric field control approaches. Using these platforms, we examine improvements in intracellular analysis, cellular engineering, drug delivery, and cell sampling to illustrate state-of-the-art RE applications. Finally, we outline future directions and trends for RE systems aimed at molecular mechanism mapping and personalized precision medicine, emphasizing their increasing relevance in practical settings.

Yuhao Zhou, Zhihui Zhang, and Feng Liu have contributed equally to this work.

✉ Yang Wang
wangyang2022@buaa.edu.cn

✉ Zaizai Dong
dongzaizai@buaa.edu.cn

✉ Lingqian Chang
lingqianchang@buaa.edu.cn

[1] Key Laboratory of Biomechanics and Mechanobiology, Ministry of Education, School of Engineering Medicine, Beihang University, Beijing 100191, China

[2] School of Biological Science and Medical Engineering, Beihang University, Beijing 100191, China

[3] Qingdao Research Institute, Beihang University, Qingdao 266100, China

**Graphical abstract**

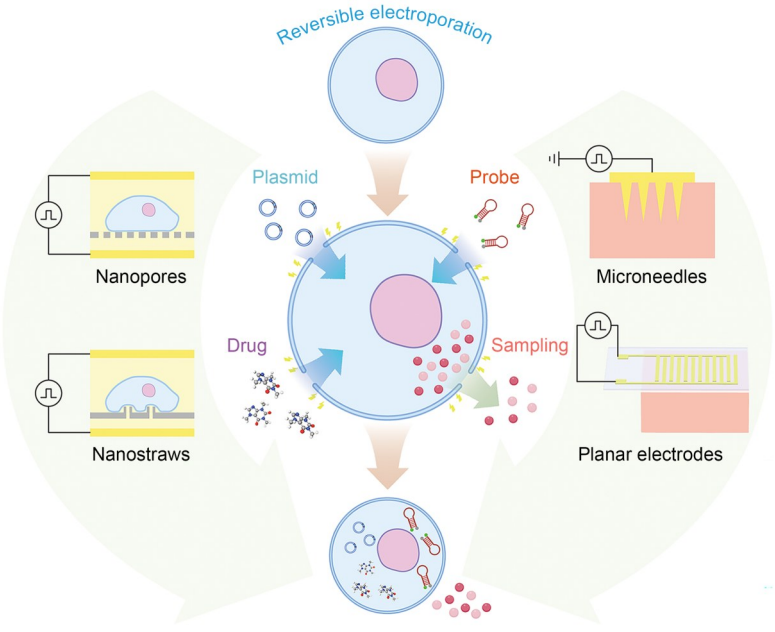


**Keywords** Reversible electroporation · Biochip · Cell analysis · Gene/Drug delivery · Cell sampling

## 1 Introduction

The cell membrane acts as a selective barrier that tightly regulates substance exchange between intracellular and extracellular environments, a role essential for sustaining cellular homeostasis [1–3]. However, this barrier also imposes dual restrictions on the efficient entry of exogenous molecules and the nondestructive extraction of intracellular substances, thereby limiting detailed mechanistic studies and functional engineering [4–8]. Therefore, creating controllable transmembrane channels that permit molecular transport while maintaining cell viability remains a central challenge [9, 10].

Reversible electroporation (RE), a cell manipulation method, uses regulated electric pulses to briefly increase cell membrane permeability, producing nanoscale pores that permit molecular exchange without inducing lasting damage [11–13]. With refined electric field control, advances in RE-integrated micro- and nano-devices have driven substantial improvements in delivery efficiency, cell throughput, and operational precision [14, 15]. For instance, nanopore-enabled RE chips achieve highly efficient and safe probe transport across tens of thousands of individual cells simultaneously [16, 17]. Moreover, coupling RE with flexible electronic microchips is broadening its applications to real-time diagnosis and in vivo therapies [18].

In this review, we describe developments in RE technology. First, we examine the electroporation process under pulsed electric fields and identify key parameters governing RE performance and safety, providing a theoretical framework for understanding interactions between operational settings and cellular behavior. We then present the design, fabrication, and optimization of RE devices, emphasizing novel micro- and nanostructured electroporation platforms that enhance efficiency through controlled electric field distribution. Furthermore, we highlight diverse RE applications enabled by regulated transmembrane transport, including intracellular analysis, cell engineering, drug delivery, and cell sampling. Finally, we discuss the strengths and limitations of current RE systems and outline future directions involving molecular mechanism profiling and personalized precision medicine. Overall, this review offers guidance to support continued advances in biological research and translational medicine.

## 2 Mechanisms of reversible electroporation

In RE, electric pulses are applied to generate transient hydrophilic pores in the plasma membrane, enabling short-term bidirectional molecular transport across the membrane [19–22]. When the pulse ends, these pores contract and reseal within seconds to minutes, restoring membrane integrity and preserving cell viability [23–26]. This process occurs in three phases: (1) pre-perforation, involving transmembrane voltage induction; (2) perforation, involving pore nucleation and expansion

accompanied by molecular transport; (3) post-perforation, involving pore closure and membrane resealing (Fig. 1).

## 2.1 Pre-perforation stage

Without an external field, the plasma membrane maintains a transmembrane potential from −40 to −70 mV that serves as a barrier to hydrophilic molecules [27]. When an electric field is applied, charged particles accumulate on both sides of the bilayer, increasing the transmembrane voltage ($\Delta V_m$). Once $\Delta V_m$ exceeds a critical threshold, pores may form in the membrane. For a spherical cell in a uniform field, the Schwan equation provides a quantitative description of this behavior [28]:

$$\Delta V_m(\theta, t) = \frac{3}{2} E R_c \cos\theta \left(1 - e^{-t/\tau_m}\right), \tag{1}$$

$$\tau_m = \frac{R_c \varepsilon_m}{\left[2d\left(\frac{\sigma_i \sigma_e}{\sigma_i + 2\sigma_e}\right)\right] + R_c \sigma_m}. \tag{2}$$

In Eq. (1), $E$ denotes the applied field strength, $R_c$ is the cell radius, $\theta$ is the polar angle relative to the field axis, and $\tau_m$ is the membrane charging time constant. In Eq. (2), $\varepsilon_m$ is the membrane permittivity, $d$ is the membrane thickness, and $\sigma_i$, $\sigma_e$, and $\sigma_m$ are the conductivities of the intracellular medium, extracellular medium, and membrane, respectively. Because induced $\Delta V_m$ scales with $\cos\theta$, it peaks at the poles ($\theta$=0° and 180°). Thus, membrane regions facing the electrodes experience the strongest electrical stress and are most likely to initiate pores, whereas equatorial regions perpendicular to the field are minimally affected.

## 2.2 Perforation stage

When $\Delta V_m$ exceeds an approximately 0.2–1.0 V threshold, the cell membrane becomes highly prone to pore formation. Field-oriented water molecules align in single-file chains along the electric field and penetrate the lipid bilayer's hydrophobic core, generating transient defects [23]. These defects serve as nascent pores and rapidly induce lipid headgroup reorientation, stabilizing hydrophilic nanopores [29]. This molecular rearrangement occurs within nanoseconds to microseconds and differs fundamentally from slower, energy-dependent membrane remodeling governed by cytoskeletal dynamics [30].

### 2.2.1 Pore nucleation

As $\Delta V_m$ increases, pore formation accelerates nonlinearly; even moderate voltage rises can produce sharp increases in pore count. However, this rapid growth is short-lived, as available nucleation sites become saturated and the effective local field declines as charge accumulates [31, 32]. The Smoluchowski-type rate equation is a commonly used mathematical model describing this process [32–35]:

$$\frac{dN}{dt} = \alpha e^{(\Delta V_m/V_{ep})^2}\left[1 - \frac{N}{N_0} e^{-q(\Delta V_m/V_{ep})^2}\right], \tag{3}$$

where $\alpha$ denotes the intrinsic pore-creation rate coefficient, $N_0$ is the pore density at $\Delta V_m$=0 V, $V_{ep}$ defines the characteristic voltage scale for efficient electroporation, and $q$ is the parameter governing saturation as $N$ approaches $N_0$. This model shows that pore creation is highly dependent on the square of the transmembrane potential; thus, slight voltage increases can markedly accelerate pore formation. However, this growth does not continue indefinitely: as transmembrane potential rises, the term $\left[1 - \frac{N}{N_0} e^{-q(\Delta V_m/V_{ep})^2}\right]$ gradually approaches unity, and as pore numbers increase, the moderating factor decreases the effective nucleation rate, thereby slowing additional pore formation relative to an exponential rise. Consistent with this theoretical prediction, Bubnis and Grubmüller [36] showed that a single 1-ms pulse at 40 kV/m produced approximately $3\times10^5$ pores per cell within 1 ms. Most of these pores had approximately 1-nm radii, with only a minority expanding to tens of nanometers.

### 2.2.2 Pore expansion

After nucleation, pore expansion reflects the competition between field-driven outward electrostatic pressure and the membrane's intrinsic restoring forces [31]. The electrostatic pressure drives pore expansion, and membrane resistance

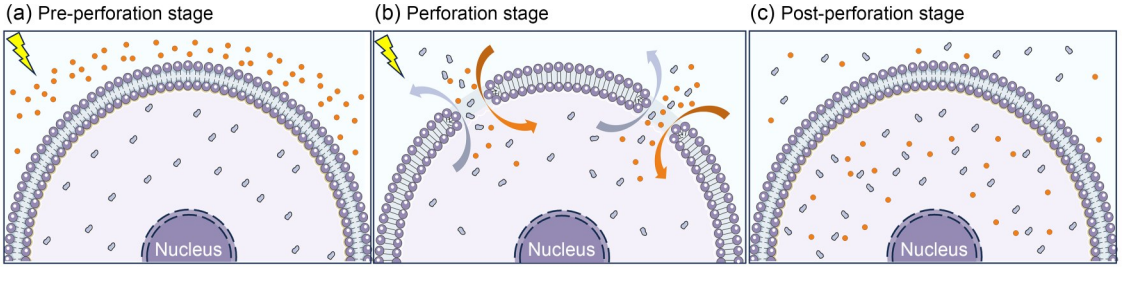


**Fig. 1** Stages of reversible electroporation. (a) Pre-perforation stage: transmembrane voltage induction. (b) Perforation stage: pore nucleation and expansion, accompanied by molecular transport. (c) Post-perforation stage: pore closure and membrane resealing

occurs through three mechanisms: surface tension, acting as an elastic restoring force that tends to limit the stretched area; line tension at the pore rim, serving as a contractile force that decreases pore circumference; and steric repulsion, which becomes dominant at subnanometer radii and prevents unphysical collapse or deformation of the pores [37–39]. Depending on the force balance, pores show three behaviors: they expand when the electric field predominates; they stabilize at an equilibrium radius when forces are balanced; they contract and reseal after external field removal when restorative forces dominate.

This process is quantitatively described within a continuum framework [40]:

$$\frac{\mathrm{d}r_\mathrm{p}}{\mathrm{d}t}=\frac{D_\mathrm{p}}{k_\mathrm{B}T}\left[\frac{F_\mathrm{max}\Delta V_\mathrm{m}^2}{1+r_\mathrm{h}/\left(r_\mathrm{p}+r_\mathrm{t}\right)}+2\pi r_\mathrm{p}\delta_\mathrm{eff}-2\pi\gamma+4\beta\left(r_*/r_\mathrm{p}\right)^4/r_\mathrm{p}\right], \tag{4}$$

where $D_\mathrm{p}$ denotes the pore-radius diffusion coefficient, $k_\mathrm{B}T$ is the thermal energy scale, and $F_\mathrm{max}$ defines the maximum electrical stress per voltage squared. The geometric factors $r_\mathrm{h}$ and $r_\mathrm{t}$ account for electric field attenuation at the pore edge. The term $\frac{F_\mathrm{max}\Delta V_\mathrm{m}^2}{1+r_\mathrm{h}/\left(r_\mathrm{p}+r_\mathrm{t}\right)}$ represents outward electrostatic pressure exerted by the applied field, which promotes pore expansion; $2\pi r_\mathrm{p}\delta_\mathrm{eff}$ captures the bilayer surface-tension contribution, reflecting membrane surface energy release with pore enlargement; $-2\pi\gamma$ indicates the line-tension penalty at the pore rim, which resists increases in rim length; $4\beta\left(r_*/r_\mathrm{p}\right)^4/r_\mathrm{p}$ accounts for the molecular-scale steric repulsion of lipid headgroups, which dominates at subnanometer pore radii, preventing collapse into unphysical pore configurations. Multiplying the algebraic sum of these forces by $D_\mathrm{p}/(k_\mathrm{B}T)$ yields effective pore mobility, where positive and negative values promote pore expansion and closure, respectively. Combined with nucleation kinetics, the continuum model helps predict pore lifetime, spatial distribution, and membrane permeability under various electroporation settings, including changes in pulse waveform, duration, and electrode geometry.

#### 2.2.3 Molecular transport

During the membrane permeabilization window, molecular transport occurs mainly via diffusion, where neutral molecules move passively along concentration gradients, and electrophoresis, where charged molecules are driven by the electric field. The Nernst–Planck equation describes this process, integrating three possible driving forces: diffusion driven by concentration gradients, electrophoretic drift governed by electric fields, and convective transport in the presence of bulk flow. When pore dimensions approach molecular size or when large polymers are transported, model corrections are required to incorporate steric effects, reduced mobility, and conformational constraints. The Nernst–Planck equation's general form is given as follows [41, 42]:

$$J_i=-D_i\nabla c_i-\frac{z_iD_iF}{RT}c_i\nabla\Phi+c_iv, \tag{5}$$

where $J_i$ denotes molar flux, $D_i$ is the diffusion coefficient, $c_i$ represents concentration, $z_i$ denotes valence, $F$ is Faraday's constant, $R$ represents the gas constant, $T$ denotes absolute temperature, $\Phi$ is the electric potential, and $v$ denotes the bulk fluid velocity. The term $-D_i\nabla c_i$ represents Fickian diffusion, whereas $\frac{z_iD_iF}{RT}c_i\nabla\Phi$ describes electrophoretic drift. In the absence of bulk flow, convection becomes negligible, reducing transport to a balance between diffusion and electrophoretic drift.

### 2.3 Post-perforation stage

After the external electric field is removed, the induced transmembrane potential collapses rapidly, and the transient aqueous pores in the membrane begin closing [43]. For small pores, resealing typically occurs through spontaneous lipid rearrangement, an energy-independent process usually completed within a few seconds. Conversely, larger or more persistent defects (often termed large or long-lived pores) may require tens of seconds to several minutes to reseal and depend on active, $Ca^{2+}$-driven repair pathways [44].

During persistent pore repair, $Ca^{2+}$ influx acts as the primary trigger. Elevated cytosolic $Ca^{2+}$ levels promote fusion of lysosome-derived and other intracellular vesicles with the plasma membrane, supplying repair components and extra membrane material [45]. In parallel, acid sphingomyelinase secretion induces membrane invagination and endocytic removal of damaged regions. Repair proteins, including annexins, dysferlin, and mitsugumin 53, are also recruited to the wound margin, where they cooperate with the actin cytoskeleton to build a contractile scaffold supporting final closure [45, 46]. Consequently, most mammalian cells restore plasma membrane integrity within seconds to minutes, with repair time varying according to electroporation intensity, temperature, and membrane fluidity [18, 47].

### 2.4 Key parameters for effective and safe RE

According to the preceding analysis of RE, the electric field around the cell and the surrounding environmental conditions shape the efficiency of cellular electroporation and subsequent molecular transport. The electric field is primarily governed by three parameters: voltage amplitude, pulse duration, and pulse count. However, environmental conditions

are mainly influenced by temperature. This subsection offers a detailed examination of these parameters, establishing a foundation for achieving efficient and safe RE outcomes [48].

#### 2.4.1 Voltage amplitude

According to the relationship $E=V/d$ and the Schwan equation, when electrode spacing is fixed, the applied voltage directly defines the electric field strength and thereby modulates $\Delta V_m$. Once $\Delta V_m$ surpasses the threshold, nanoscale hydrophilic pores emerge in the plasma membrane. Higher voltages produce more pores with larger radii, which increases the efficiency of molecular entry into cells [49−51]. For example, Brooks et al. [52] showed that DNA delivery efficiency peaked at approximately 60%–70% within a field strength of approximately 400–600 V/cm but declined rapidly outside this range. Similarly, Rols and Teissié [53] reported that raising the field strength from 200 to 600 V/cm substantially improved the uptake of fluorescent molecules but also markedly increased cell mortality.

Thus, voltage amplitude exerts a dual effect on electroporation: moderate increases promote pore formation and molecular transfer, whereas excessive voltages trigger uncontrolled pore growth, membrane integrity failure, and reduced cell viability [54, 55]. Therefore, identifying an optimal voltage range is essential to balance high delivery efficiency with cell survival.

#### 2.4.2 Pulse duration

Pulse duration determines the time available for charge redistribution across the membrane under an applied electric field, thereby affecting pore stability and size. According to the Schwan equation, when pulse duration is shorter than the membrane charging time constant ($\tau_m$), $\Delta V_m$ cannot fully develop, reducing pore nucleation. In contrast, when the duration approaches or exceeds $\tau_m$, $\Delta V_m$ nears a steady state and supports more effective pore formation and growth [25, 56]. For instance, Pavlin and Kandušer [57] found that combining long and short pulses improved gene delivery: four 200-ms high-voltage pulses followed by a 100-ms low-voltage pulse increased transfection efficiency from approximately 6% to 23% while preserving approximately 90% cell viability. Additionally, short microsecond-scale pulses (approximately 100–200 μs) generally suffice for small molecule (< 1 kDa) delivery, whereas medium-sized cargoes (approximately 10 kDa) typically require millisecond pulses, and large macromolecules, such as plasmid DNA, often need 10–50-ms pulses to enter cells effectively.

In summary, the effects of pulse duration depend on molecular size: larger molecules require longer pulses for efficient delivery. However, overly extended pulses elevate thermal load and the risk of irreversible electroporation (IRE), reducing cell viability. An optimal strategy is to tailor pulse duration to the cargo and cellular tolerance or use hybrid long–short pulse regimens that improve delivery efficiency while preserving viability.

#### 2.4.3 Pulse count

The number of pulses regulates pore formation through cumulative effects. Before pore count reaches saturation, additional pulses generate new pores, and subsequent pulses keep existing pores activated or expanding, thereby increasing overall pore density [58]. However, as nucleation sites become saturated and charge accumulation near pores alters local electric fields, the effective field strength in untouched membrane regions diminishes, limiting further pore formation. Rather than improving delivery, excessive pulses deposit excess energy and generate harmful byproducts, shifting RE toward irreversible damage [59].

Experimental studies have demonstrated that pulse trains can enhance molecular uptake while allowing partial membrane resealing during interpulse intervals, thereby lowering the risk of cell damage. For instance, Mickevičiūtė et al. [59] showed that bipolar pulse sequences promote uniform permeabilization and preserve high viability by pairing a short high-voltage pulse to form hydrophilic pores with a long low-voltage pulse to maintain openings.

Optimizing pulse count requires balancing enhanced delivery with avoidance of excessive energy deposition. Using a moderate number of pulses with well-designed waveforms, such as bipolar sequences, represents a practical method for improving delivery outcomes while minimizing adverse effects.

#### 2.4.4 Temperature

Temperature, a key environmental variable, influences electroporation efficiency and cell viability by altering membrane fluidity, pore formation thresholds, and resealing kinetics [60]. At lower temperatures, lipid mobility decreases and pore closure slows, extending the transport window but raising the $\Delta V_m$ required for pore formation. At physiological or elevated temperatures, membranes become more deformable and reseal faster, improving cell survival but shortening the permeabilization window. Under high-energy pulse regimens, elevated temperatures may further exacerbate cellular stress via excessive membrane fluidity, protein denaturation, or oxidative damage [61]. For example, Kandušer et al. [60] reported that lowering the electroporation temperature from 37 to 4 °C halved the permeability of cells under otherwise identical pulse conditions, highlighting the strong regulatory effect of temperature on membrane dynamics and molecular transport efficiency. In summary, temperature exerts a dual effect on electroporation: low temperatures extend

transport duration but raise pore formation thresholds and may cause additional injury during rewarming, whereas higher temperatures support cell survival but shorten delivery opportunities. Maintaining physiological temperatures or making only mild adjustments while monitoring and controlling thermal conditions helps ensure reproducibility and effective RE performance [62].

Systematic optimization of the aforementioned parameters is essential for establishing suitable electroporation conditions (Fig. 2). Particular emphasis should be placed on electric field strength and pulse duration, as both govern the boundary between RE and IRE (Table 1). RE is typically induced by lower field strengths (e.g., 0.2–1.0 kV/cm) and shorter pulses (microseconds to milliseconds), generating transient nanopores that reseal and maintain cell viability [63]. In contrast, IRE relies on markedly higher field strengths (>0.8 kV/cm) and/or longer pulses, which produce widespread irreversible pore formation that disrupts cellular homeostasis and induces cell death [50]. This boundary also depends on factors such as cell type, temperature, and buffer conductivity [64]. Thus, precise control of these parameters is crucial to achieve sufficient permeabilization while minimizing cytotoxicity. Besides direct parameter tuning, advances in micro- and nanoscale electroporation technologies, including microfluidic and chip-based systems, have provided powerful platforms for improved control of the RE process.

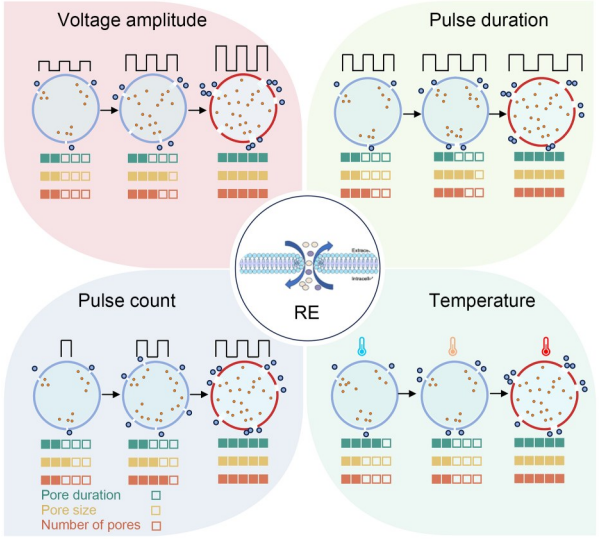


**Fig. 2** Effects of voltage amplitude, pulse duration, pulse count, and temperature on pore formation and transport dynamics during reversible electroporation (RE)

## 3 Electric field control method for RE

Precise modulation of the electric field enables highly efficient and safe membrane electroporation, establishing a critical technological foundation for advanced cellular diagnostics and genetic engineering. Advances in RE-enabled devices have enabled fine manipulation of electric fields, providing a promising direction for future research.

Conventional RE devices, typically based on bulk cell electroporation instruments, consist of a main unit that controls electrical pulse parameters and a specialized cuvette that generates the electric field. Electric field regulation is usually achieved by directly adjusting pulse settings, including voltage, pulse width, and pulse count. Although these instruments can introduce exogenous molecules into cells, their relatively coarse electric field control limits the ability to simultaneously achieve both high delivery efficiency and cell viability.

In contrast, RE devices integrated with micro- and nanostructures have been developed to achieve precise electric field control. These devices modulate the electric field distribution around cells, enabling elevated delivery efficiency and viability. Based on their structural mechanisms of electric field distribution, newly developed micro- and nano-devices for RE can be categorized into five major types: microfluidic chips, nanopore-based chips, nanostraw-based chips, microneedle patches, and electrode array-based chips.

### 3.1 Microfluidic chips

Microfluidic electroporation devices employ microchannels as the electroporation region and integrate electrodes to apply electric fields. Within these microchannels, the distance between electrodes and cells is reduced to the micron scale, and the electric field is tightly confined, substantially minimizing field attenuation [70]. Additionally, multiple cells pass

**Table 1** Comparison of key operating parameters distinguishing RE from IRE

| Parameter | RE | IRE | Ref. |
|---|---|---|---|
| $\Delta V_m$ | 0.2–1.0 V | >1.0 V | [50, 63, 64] |
| Electric field strength | 200–800 V/cm | >800 V/cm | [65, 66] |
| Pulse duration | 10 μs–10 ms | 50–100 μs | [67] |
| Pulse count | 1–10 pulses | >80 pulses | [44, 66, 68] |
| Repetition rate | 1–5 Hz | 1–4 Hz | [69] |

RE: reversible electroporation; IRE: irreversible electroporation; $\Delta V_m$: transmembrane voltage

through the narrow microchannels at the same flow rate under a uniform electric field, ensuring consistent RE effects across the entire population and eliminating batch-to-batch variation. Furthermore, the hydrodynamic environment in the microchannels maintains fluid flow during electroporation, protecting cells from thermal accumulation and prolonged high-field exposure.

Microfluidic electroporation devices are typically fabricated using polydimethylsiloxane casting and bonding processes. Electrodes positioned on both sides of the microchannels allow electric fields to fully cover the channel region. Platinum wire electrodes are favored in microfluidic chips because they do not release harmful metal ions under high voltage. Dong et al. [71] used nanosecond pulses to open the organelle membranes of flowing cells, facilitating plasmid entry into the nucleus and activating pathways related to small extracellular vesicle (sEV) secretion (Fig. 3a). Compared with traditional systems, this approach increases sEV secretion by >30-fold while reducing damage to nontarget cells.

In addition to silicone-based microchannels, hollow tubing is widely used in microfluidic RE devices owing to its simple fabrication and strong scalability. Electrodes are

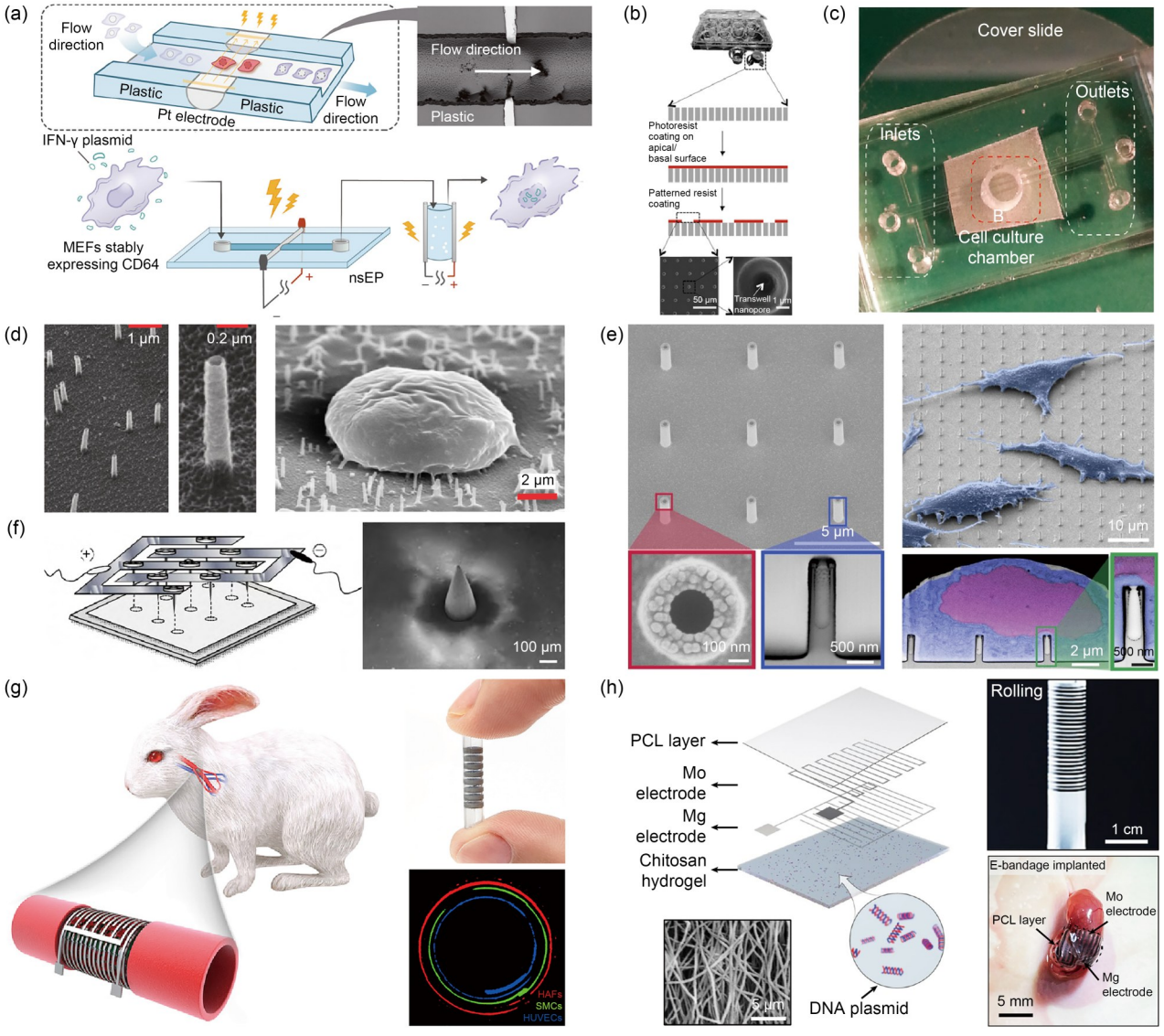


**Fig. 3** Reversible electroporation (RE) devices and structures. (a) Bulk electroporation using a platinum wire electrode (reproduced from [71], licensed under CC BY 4.0). (b) Large-scale transfection at single-cell resolution enabled by heterogeneous nanopores (reproduced from [76], with permission from Elsevier Inc.). (c) Microfluidic chip supporting long-term cell culture and repeated transient electroporation (reproduced from [78], with permission from The Royal Society of Chemistry). (d) Hollow alumina nanostraws (reproduced from [79], licensed under CC BY-NC-ND). (e) Electroactive nanoinjection (ENI) platform using vertically configured conductive nanotubes (reproduced from [80], licensed under CC BY 4.0). (f) In-skin electroporation via microneedle electrode arrays (reproduced from [81], with permission from Elsevier B.V.). (g) Electronic blood vessel enabling site-specific gene delivery through localized electroporation (reproduced from [98], with permission from Elsevier Inc.). (h) Self-powered electronic bandage providing dual electrostimulation for enhanced wound healing (reproduced from [99], under exclusive licence to Springer Nature Limited)

positioned at both ends of the tubes, and an alternating electric field is generated using an external power supply or a triboelectric nanogenerator (TENG). Using such a device, Liu et al. [72] delivered 40-kDa fluorescein isothiocyanate (FITC)-dextran into cells while maintaining >90% cell viability. Huang et al. [73] investigated the relationships among fluid velocity, electric field intensity, and cell viability in the device, identifying an optimal residence time of 5 ms.

In summary, microfluidic electroporation chips provide a uniform electric field to every cell, are simple to fabricate, and are convenient to operate, making them powerful tools for high-throughput cell processing. However, when more precise electric field control is required, channel clogging, especially by large cell clusters or primary cells with irregular morphologies, can impair device function and reduce processing efficiency. Balancing precise control with high throughput remains a key challenge for future design improvements.

## 3.2 Nanopore-based chips

Nanopore-based chips integrate a nanoscale porous membrane between a pair of parallel electrodes, with cells positioned directly on the nanopores. Most nanopores are fabricated on polymer membranes, such as polycarbonate, polyethylene terephthalate, or polyimide, using laser ablation or plasma etching. Because these membranes are insulating, the electric field preferentially conducts through the electrolyte inside the pores rather than through the membrane, leading to strong electric field enhancement at the pore edges. This configuration locally focuses the electric field onto a small region of the cell membrane attached to the nanopore, allowing electrophoretic exchange of intracellular and extracellular materials. Compared with bulk electroporation, which requires high voltages, this localized electroporation achieves efficient delivery at only 10–25 V, minimizing Joule heating and membrane damage.

Leveraging these electric field characteristics, nanopore-based chips can achieve efficient electroporation and targeted molecular delivery while maintaining high cell viability. For example, Ma et al. [74] used polycarbonate nanopore membranes to deliver plasmid DNA into human adipose-derived mesenchymal stem cells, achieving 75% transfection efficiency with 75% cell survival. Dong et al. [75] developed an electroporation chip using engineered pore geometries to enhance directional field focusing, achieving >90% delivery and 90% cell survival at low voltages (10–25 V).

To further enhance RE efficiency, researchers have refined nanopore configurations. Gallego-Perez et al. [76] optimized nanopore size to regulate electric field gradients and control plasmid dosage, enabling large-scale, uniform transfection with single-cell resolution (Fig. 3b). Pathak et al. [77] combined 200-nm nanopores with a bipolar pulse protocol to simultaneously improve delivery efficiency and cell activity.

Integration with microfluidic systems further enhances the electric field control effect by promoting the electrophoretic transport of charged molecules. Kang et al. [78] integrated a nanopore membrane with microelectrodes on both sides of a microchannel (Fig. 3c), with their channel design ensuring uniform cell flow across the pore surface, providing consistent delivery efficiency. This platform also supports long-term cell culture and repeated transient transfection, maintaining cell viability above 85% after multiple treatments.

In conclusion, nanopore-based chips support efficient molecular delivery to large numbers of cells while maintaining high viability. Their compatibility with microfluidic systems offers broad potential for applications in cell analysis and engineering. However, because efficient nanopore electroporation requires cells to be in close contact with the membrane, performance is limited for weakly adherent or loosely attached cells, reducing applicability across certain cell types.

## 3.3 Nanostraw-based chips

Nanostraw-based chips for RE feature hollow, high-aspect-ratio nanochannels that concentrate the electric field into an extremely small region at the nanostraw tips while minimizing field diffusion to nontarget areas. This concentration, amplified by curvature-induced edge effects, generates a localized high-intensity electric field that enables effective membrane electroporation and molecular delivery at low applied voltages. Nanostraw devices are typically fabricated using continuous thin-film processes: aluminum oxide is first conformally deposited onto a polymer film via atomic layer deposition or plasma-enhanced chemical vapor deposition, followed by anisotropic reactive ion etching to define pore size and oxygen plasma etching to release the nanostructures.

The oriented nanostraw architecture directs the electric field and molecular transport, ensuring that charged molecules pass through the nanochannels and enter the cytoplasm under electrophoretic forces. Several studies have validated the advantages of nanostraw structures. For example, Schmiderer et al. [79] engineered aluminum oxide nanostraws with an inner cavity measuring 100 nm, markedly enhancing electric field confinement at the tip (Fig. 3d). This structural optimization enabled the delivery of 2000-kDa dextran molecules into cells using a low-power pulsed field.

Nanostraw chips also maintain higher cell viability relative to bulk electroporation systems owing to their highly localized field distribution, which restricts membrane permeabilization to the immediate vicinity of the nanostraw tips. Shokouhi et al. [80] employed vertically aligned conductive nanostraws that achieved an edge electric field strength of 1.5 kV/cm under an input voltage of 5 V (Fig. 3e). Using this platform for small interfering RNA (siRNA) delivery, they achieved a gene knockout efficiency of 41.3% while preserving high cell viability.

In conclusion, nanostraws effectively confine electric fields and provide directed channels for molecular transport. Their compatibility with a variety of physical and chemical delivery modalities further enhances synergistic effects in the transfection of biomolecules, such as DNA, supporting the development of cell therapy and gene editing technologies. However, a fundamental limitation of nanostraw-based chips lies in their restricted physical length, which prevents effective penetration into three-dimensional cellular aggregates or thick tissues. This geometric constraint reduces their suitability for in vivo RE but also confines their application primarily to two-dimensional culture systems.

### 3.4 Microneedle patches

Microneedle patches leverage high-aspect-ratio conductive arrays to enhance electric field intensity at the target site while limiting the spatial extent of its influence. By integrating conductive microneedle arrays, these devices can penetrate tissue matrices and establish direct electrical contact with cells located beneath the surface. When voltage is applied, charge preferentially accumulates at regions of high curvature, resulting in a substantially higher charge surface density at microneedle tips. Compared with planar electrodes, microneedles reduce the required voltage by 1–2 orders of magnitude and avoid electric field attenuation within bulk tissue, ensuring that deeper cells achieve sufficient transmembrane potential for effective electroporation. The confined electric field also minimizes nonspecific permeabilization of adjacent cells and reduces collateral damage.

For transdermal applications, microneedle patches bypass the high-impedance stratum corneum and deliver a concentrated electric field directly to the viable dermis. The targeted field distribution increases the delivery efficiency of DNA vaccines and clustered regularly interspaced short palindromic repeats (CRISPR) ribonucleoproteins by 3–5-fold relative to surface electrode systems. Yan et al. [81] developed high-aspect-ratio microneedle electrode arrays (Fig. 3f), which simultaneously pierce the skin barrier and function as electrodes to apply electric fields within the tissue. This technique enhances deep macromolecular drug delivery by inducing transient electroporation and creating permeation pathways, achieving >7-fold higher transdermal dextran delivery compared with conventional on-skin electroporation.

Conductive hydrogel materials, with strong plasticity and biocompatibility, have also emerged as promising candidates for microneedle fabrication. Wang et al. [82] designed a pyramid-shaped microneedle array possessing DNA-loaded tips, with DNA release driven by iontophoresis at a low voltage of 1 V, followed by the application of a 90-V pulsed voltage generating an electric field strength >400 V/cm near the electrode tips. By combining hydrogels with microneedle structures, this device improves skin permeability while minimizing irritation.

In summary, microneedle patches effectively overcome electric field attenuation in tissues, expanding the application landscape of RE and providing a feasible approach for implementing electroporation in wearable devices and in vivo systems. However, despite their biocompatibility, microneedle penetration inevitably causes localized tissue damage. Such trauma can trigger inflammatory responses that may compromise the local microenvironment and interfere with the long-term repeatability of RE treatments.

### 3.5 Electrode array-based chips

A key structural feature of electrode array-based chips is the miniaturization of electrode size and interelectrode spacing to the micro- and nanoscale. This configuration enables the generation of high electric field intensities at ultra-low voltages, producing a predominantly transverse field confined parallel to the electrode plane. Such spatial confinement supports effective electroporation of superficial tissues, including epidermal and corneal layers, while minimizing damage to deeper cells [83].

Electrode array-based chips are typically fabricated using micro-electro-mechanical system processes or screen printing, allowing consistent replication of nanoscale features and high reproducibility of electric field characteristics across devices [84]. Efficient transmembrane electroporation also requires minimizing perturbations from electrochemical reactions [85]. Two complementary strategies, geometric optimization and material selection, can reduce electrode impedance and are readily integrated into the fabrication process [86]. Geometric strategies increase effective surface area through electrodeposition of nanostructured materials, such as carbon nanotubes, or conductive powders, including platinum black [87]. For instance, Gharia et al. [88] developed rough-surfaced poly(3,4-ethylenedioxythiophene) (PEDOT): polystyrene sulfonate (PSS) electrodes that increase contact area at the electrode–tissue interface, preventing localized heating and excessive field concentration caused by poor contact. Concurrently, materials with high charge-injection capacity and low impedance, including activated iridium oxide and titanium nitride, further reduce irreversible Faradaic reactions and gas evolution [89]. Lin et al. [90] fabricated iridium oxide nanotube electrodes exhibiting high capacitance without inducing redox reactions, while supporting prolonged intracellular pathway activity. Collectively, these approaches lower the voltage required for effective electroporation while improving efficiency and biocompatibility.

The interdigitated electrode represents a common example of controlled electric field modulation in electrode array-based chips [91]. Its alternating finger-like coplanar layout

generates uniform, localized electric fields within the narrow electrode gaps, restricting electroporation to cells within these regions. Combining such electrodes with microfluidic systems enhances control precision. Ouyang et al. [92] aligned planar electrodes with microchannel flow paths, ensuring that cells traverse the optimal field zone. Segmenting microchambers to correspond with individual electrode pairs further stabilizes current distribution and improves electroporation consistency by isolating field regions [93, 94].

Flexible planar electrodes extend RE to curved biological surfaces [95, 96]. Fabricated as micro-electro-mechanical systems (MEMS) on biocompatible polymer substrates, these electrodes conform to irregular tissue geometry and ensure uniform field delivery through close contact. For example, the carbon nanotube mask developed by Xu et al. [97] forms conformal contact with skin to enhance nicotinamide delivery via controlled electroporation, enabling transdermal application.

When integrated with flexible materials, electrode array chips demonstrate advantages for in vivo applications. Cheng et al. [98] developed an "electronic blood vessel" incorporating thin-film electrodes into vascular grafts, enabling site-specific gene delivery by confining the electric field to selected vascular segments while preserving >90% patency post-implantation (Fig. 3g). Degradable thin-film designs, such as the Mg/Mo electrode developed by Wu et al. [99], introduce temporal control over field application (Fig. 3h). These magnetron-sputtered electrodes gradually degrade after triggering intestinal epithelial transfection, eliminating sustained field exposure and reducing adverse reactions.

Overall, electrode array-based chips offer geometric versatility, scalability, and conformability, establishing them as robust platforms for diverse in vivo applications. Their compatibility with flexible materials and integration potential with artificial intelligence further enhances functionality, supporting advanced biosensing and precision therapeutic systems. Despite these advantages, both degradable and permanent arrays face biostability challenges that limit repeated RE. Degradable electrodes exhibit unpredictable performance decay, whereas nondegradable electrodes show impedance increases due to fibrous encapsulation and biofouling, collectively impairing electric field delivery and long-term reliability.

Based on their electric field control capabilities, these RE platforms exhibit broad applicability in both in vitro and in vivo contexts (Table 2). Microfluidic chips, nanopore-based chips, nanostraw-based chips, and electrode array-based chips are widely used in vitro for precise molecular delivery under controlled conditions. Several device types, including nanopore-based chips, microneedle patches, and electrode array-based chips, have also demonstrated strong potential for in vivo delivery, enabling localized and minimally invasive electroporation in living tissues. Section 4 highlights the practical applications of these devices and illustrates their translational relevance from bench to bedside.

## 4 Molecular control applications of RE

Controlled membrane permeabilization provides directional propulsion for charged molecules, enabling precise intracellular delivery, extraction, and sampling. This propulsion mirrors electrophoretic forces in biological assays, where positively and negatively charged species migrate toward the negative and positive electrodes, respectively. Therefore, by configuring electrode polarity and placement, RE enables regulated transport of charged molecules either into the cell or outward for sampling. Based on the molecular type, such as probes, nucleic acids, drugs, or intracellular components,

**Table 2** Comparison of key parameters and performance across reversible electroporation device types

| Type | | Parameter range | Delivery efficiency | Cell/Tissue viability | Cell throughput | Advantages | Limitations | Ref. |
|---|---|---|---|---|---|---|---|---|
| In vitro | Microfluidic chips | 50–200 V; 0.5–5 ms | >90% | >90% | Medium | Easy to operate, low cost | Cell size limitation | [71, 72, 100] |
| | Nanopore-based chips | 10–100 V; 0.25–2 s | 75%–95% | >90% | High | Low cell damage, broad range of delivery types | Pore size limitation | [74, 76–78] |
| | Nanostraw-based chips | 5–40 V; 0.2–0.4 ms | >60% | >89% | High | Low voltage, accurate transmission | Cell invasive injury | [79, 80, 101] |
| | Electrode array-based chips | 5–150 V; 0.1–200 ms | 70%–90% | >80% | High | High spatial resolution, miniaturizable | High degradation requirement | [83, 93–95] |
| In vivo | Nanopore-based chips | 20–50 V; 20 ms | 90%–98% | No damage | High | Broad range of delivery types | Lack of organ suitability | [102] |
| | Microneedle patches | 30–50 V; 10–100 ms | >50% | >90% | High | Minimally invasive, painless, efficient targeting | Tissue damage | [81, 82] |
| | Electrode array-based chips | 30–200 V; 1–100 ms | 30%–95% | >90% | High | High biocompatibility, high fitness | Implantable, degradable requirements | [97–99] |

RE applications can be categorized into intracellular detection, cell engineering, drug delivery, and cellular sampling.

### 4.1 Intracellular detection

Each cell contains approximately 8000–12 000 RNA species and approximately 10 000–20 000 protein types, collectively governing behaviors such as proliferation, migration, and stress responses [103–105]. Sensitive detection of these molecules requires transient membrane permeabilization and accurate intracellular detection tools. For RE-mediated intracellular detection, current approaches primarily rely on two probe classes: fluorochromes and DNA probes [106–108].

Fluorochromes, such as propidium iodide (PI), a red fluorescent dye used to assess cell viability, are commonly used to optimize RE conditions. PI cannot passively cross intact membranes but readily enters cells during electroporation, where its positive charge promotes rapid influx and signal activation. When PI is combined with calcein acetoxymethyl ester (calcein-AM), used to evaluate cell viability through green fluorescence, the proportion of successfully transfected and viable cells can be quantified via dual-staining analysis. These dyes are inexpensive with high fluorescence efficiency but exhibit limited molecular specificity, restricting their ability to identify particular biomolecules.

To achieve molecular specificity, negatively charged DNA probes can be delivered by RE for real-time analysis of intracellular RNA and protein targets [109]. For RNA detection, DNA probes hybridize with target transcripts via complementary base pairing, displacing paired strands and initiating downstream signal transduction. For example, Chang et al. [110] used RE to deliver molecular beacons into leukemia cells for *GATA2* transcript detection. Molecular beacons are stem-loop oligonucleotides conjugated with fluorophore–quencher pairs; binding to target RNA separates the fluorophore from the quencher and restores fluorescence, enabling quantitative RNA measurement. However, molecular beacons are susceptible to intracellular nuclease degradation, compromising detection accuracy. To improve stability, Dong et al. [111] engineered a tetrahedral DNA probe (DNAT) targeting programmed death-ligand 1 (PD-L1), glyceraldehyde-3-phosphate dehydrogenase (GAPDH), and cytokeratin (CK) mRNAs (Fig. 4a). The rigid three-dimensional architecture provides nuclease resistance and enhances detection accuracy. Integrated with a microfluidic chip, DNAT probes were delivered into circulating tumor cells (CTCs) by RE with high efficiency (95%) and cell viability (90%). Through subsequent coculture of CTCs and immune cells, a novel predictive index, the nanoplatform for interrogating living cell host-gene and (micro-)environment (NICHE, the ratio of CTCs with high PD-L1 expression and lengthened phenotype) was proposed for evaluating lung cancer immunotherapy response, improving diagnostic accuracy from 0.578 to 0.906.

Given the low abundance of many intracellular molecules, multiple cooperative probes are often required to amplify

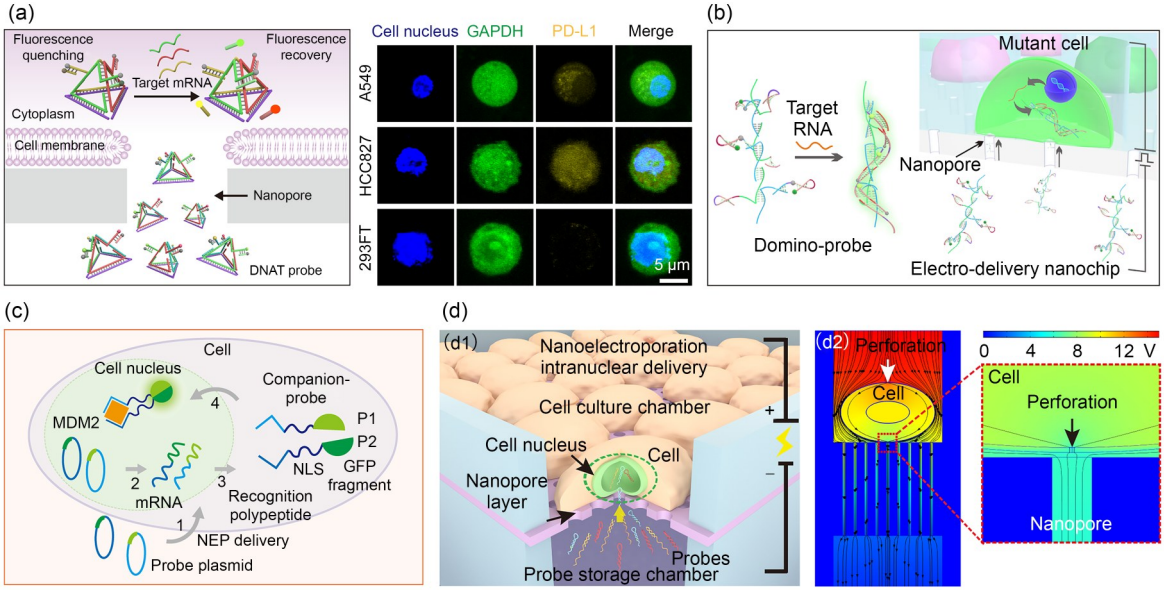


**Fig. 4** Intracellular detection enabled by RE-based probe delivery. (a) DNAT probes delivered by RE into living CTCs for quantifying intracellular mRNA expression. Fluorescent images show DNAT-labeled cells (reproduced from [111], licensed under CC BY 4.0). (b) Domino probes delivered by RE for identification of mutant RNAs (reproduced from [112], with permission from the American Chemical Society). (c) Plasmids encoding dual peptide probes for specific nuclear protein recognition (reproduced from [113], with permission from Elsevier B.V.). (d) RE delivers plasmids encoding probe pairs: (d1) RE-mediated nuclear delivery of probes for detecting enhancer activity; (d2) simulated electric fields show electrophoretic forces that drive probe entry into the nucleus after membrane electroporation (reproduced from [114], with permission from the American Chemical Society)

signal output. RE excels at multiplexed probe delivery, achieving rapid and uniform probe loading within seconds. Dong et al. [112] developed a "Domino" probe for signal amplification (Fig. 4b). Delivered via RE into thousands of single cells with >90% efficiency and viability, Domino probes reduced the total cell analysis time to <30 min, substantially faster than the 4–24 h required by conventional incubation-based delivery methods.

For protein detection, aptamers, also referred to as "chemical antibodies," are used to recognize specific proteins. One strategy involves using plasmids encoding peptide aptamer probes produced via endogenous cellular expression (Fig. 4c) [113]. RE delivers plasmids encoding probe pairs that incorporate three functional elements: (1) a protein-recognition polypeptide, (2) nuclear localization signals, and (3) green fluorescent protein (GFP) fragments. Binding of the two probe components to the target nuclear protein reconstitutes GFP fluorescence, enabling quantitative measurement of protein abundance as well as real-time tracking of protein expression and cell migration. Additionally, residual electrophoretic field forces following membrane permeabilization can facilitate nuclear import through nuclear pore complexes, a phenomenon validated experimentally and applied to enhancer activity within the cell nucleus (Fig. 4d) [114].

A critical factor for intracellular detection accuracy is the amount of delivered probe; inconsistent loading leads to signal fluctuations and quantitative errors. A major challenge in achieving uniform probe delivery via RE is inherent cellular heterogeneity, i.e., variations in cell size, membrane composition, and gene expression, even within clonal populations [115]. These differences alter membrane stability and electrophysiological properties [116], producing heterogeneous electroporation outcomes. Advanced technologies address this limitation through single-cell RE platforms and intelligent feedback-controlled systems. For example, microfluidic platforms with isolated chambers enable cell-specific parameter tuning by eliminating intercellular crosstalk and reducing electric field heterogeneity [93]. Complementarily, deep learning models trained on multi-omics datasets can predict optimal pulse parameters from cellular features [117]. A model trained on >10 000 cells achieved >85% delivery uniformity across five cell types by dynamically adjusting parameters based on cell diameter and membrane capacitance, markedly outperforming fixed-parameter approaches. These technologies enable real-time monitoring and adaptive control, improving delivery consistency and strengthening quantitative intracellular analysis.

## 4.2 Cell engineering

RE enables the introduction of exogenous genetic material into target cells for efficient gene transfection, thereby supporting diverse cell-engineering applications. Delivered genetic cargoes fall into two major categories: RNA- and DNA-based molecules. RNA-based agents, including siRNA, microRNA, and mRNA, are selected to downregulate or upregulate target gene expression. DNA-based regulation primarily involves plasmid delivery [118]. Plasmids are small, circular, double-stranded DNA molecules capable of autonomous replication and stable gene expression within host cells [119, 120]. Owing to its efficiency, safety, and broad applicability, RE is widely used for in vitro and in vivo cell engineering [121−123].

For in vitro cell engineering, Liu et al. [72] developed a bulk electroporation system for transfection (BEST), characterized by its simplicity, self-assembly, high throughput, and self-powered operation (Fig. 5a). Comparing RE without free-standing (FS)-TENG stimulation to stimulation at 10 and 15 Hz, the system showed substantially increased transfection efficiency under electrical modulation. BEST achieved >50% gene delivery in HeLa cells while maintaining >90% cell viability, demonstrating safe and efficient bulk electroporation.

To further enhance control over RE, the electric field distribution can be precisely regulated. Liu et al. [124] created an RE platform employing nanopore-focused electric fields (Fig. 5b), achieving delivery of genetic material with up to 93% efficiency. This system enables the genetic modification of aggressive cancer cells, noninvasively isolated from heterogeneous tumor samples. The engineered cells secrete extracellular vesicles (EVs) with improved tumor-targeting capability and therapeutic efficacy. These EVs activate immune responses in macrophages and T cells, yielding strong antimetastatic and treatment-enhancing outcomes.

For in vivo cell engineering, Yin et al. [102] developed a battery-free, soft nanofluidic patch for intracellular delivery to visceral organs (Fig. 5c). Its chip-free architecture and flexible functional layers allow seamless integration with organ surfaces, and a nanopore–microchannel–microelectrode structure provides safe, efficient, and precise electroporation. This device accelerates intracellular transport by approximately $10^5$-fold relative to conventional diffusion methods, even at low voltages (20 V). Validated across multiple in vivo contexts, including breast tumor treatment, acute liver injury therapy, and tumor development modeling, the patch enables efficient, safe, and controllable organ-targeted gene delivery [125].

A central challenge for in vivo electroporation systems is achieving controlled biodegradability without loss of electrical and mechanical function. To address this, Wu et al. [99] designed a biodegradable, flexible, self-powered electronic bandage to promote intestinal wound repair (Fig. 5d). This device employs dual-mode electrical stimulation: pulsed fields induce electrotransfection in epithelial cells and enhance the expression of healing factors (e.g., epidermal growth factor), and a magnesium–molybdenum galvanic cell provides continuous direct-current stimulation to further boost factor secretion. The electronic bandage achieves high transfection

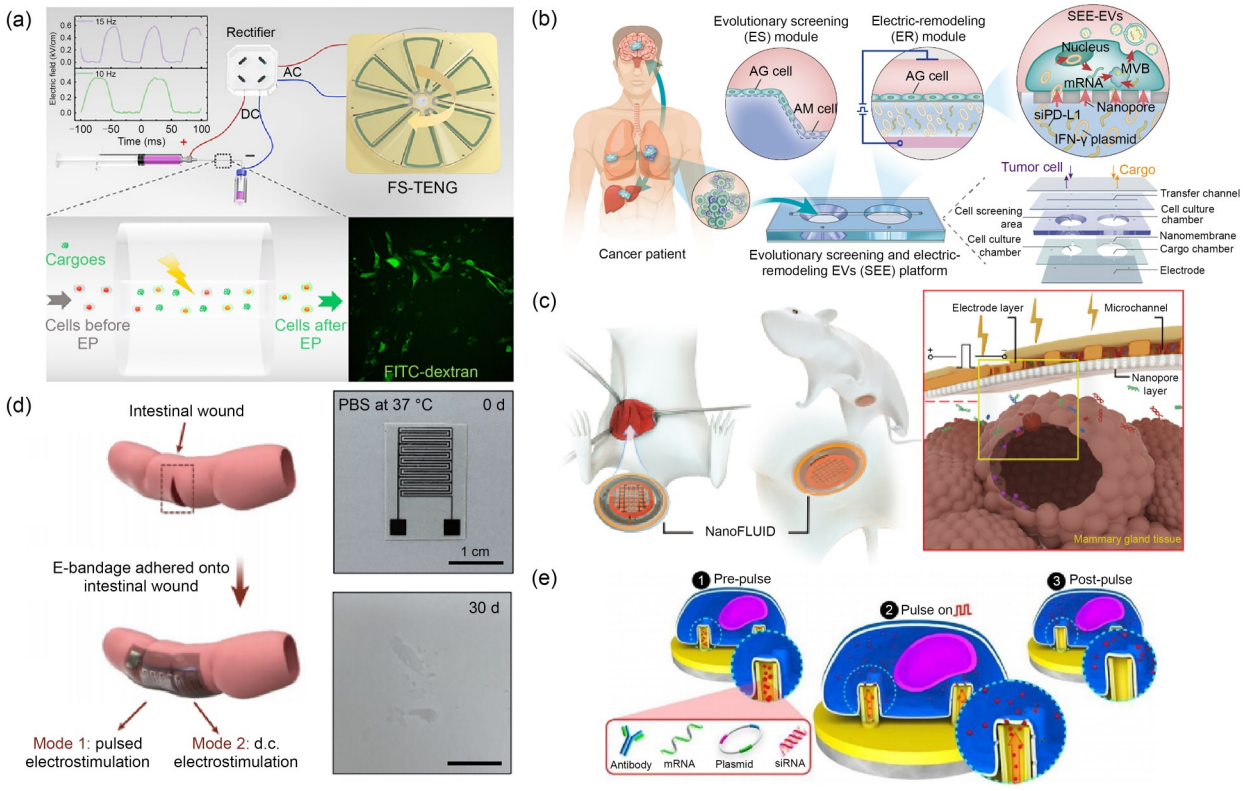


**Fig. 5** Application of RE in cell engineering. (a) High-throughput, self-powered BEST for safe and efficient gene delivery (reproduced from [72], with permission from the American Chemical Society). (b) Nanopore-focused platform for tumor cell evolution screening and RE-based genetic modification (reproduced from [124], licensed under CC BY 4.0). (c) Battery-free, flexible nanofluidic patch enabling enhanced and customizable payload delivery in visceral organs (reproduced from [102], under exclusive licence to Springer Nature Limited). (d) Self-powered, biodegradable electronic bandage for accelerating intestinal wound healing (reproduced from [99], under exclusive licence to Springer Nature Limited). (e) Low-pressure, reusable electroactive nanoinjection platform for efficient delivery of diverse macromolecules (reproduced from [80], licensed under CC BY 4.0)

efficiency and viability in vivo, increases epidermal growth factor expression during surgery, and naturally degrades after healing, eliminating the need for device removal.

Beyond genetic cargoes, RE also supports the delivery of proteins, antibodies, and other bioactive molecules, offering versatility for cell therapy development. Shokouhi et al. [80] proposed a low-voltage, reusable electroactive nanoinjection platform based on vertically aligned conductive nanotubes (Fig. 5e). This system enabled highly localized, efficient delivery of antibodies, mRNA, and plasmid DNA into mouse fibroblast cells while maintaining >90% cell viability. It also successfully achieved gene knockdown by delivering TRIOBP-targeting siRNA with 41.3% silencing efficiency, underscoring its potential for gene therapy applications.

## 4.3 Drug delivery

In RE, short, high-intensity electrical pulses are applied to form transient pores in the cell membrane, increasing permeability and enabling rapid intracellular entry of therapeutic agents. Its ultrafast operation (often <1 s) substantially shortens the prolonged drug incubation time required in traditional assays. Effective drug delivery via RE depends on two factors: (1) the drug must carry an inherent charge to permit electrophoretic transport, and (2) electroporation parameters must be precisely tuned to maintain cell viability. Achieving efficient, targeted drug delivery while ensuring biosafety remains a key research challenge.

To address this, a nanoelectroporation system incorporating DNA tension probes was developed, achieving 90% delivery efficiency, strong biosafety, and a total delivery time of only 3 s (Fig. 6a) [126]. Localized nanochannel-confined electric fields enable controlled membrane perforation and accelerate intracellular delivery by $10^3$-fold. Coupled with single-cell array chips for cellular barcoding, the system captures cellular heterogeneity and enables precise assessment of drug resistance among tumor subpopulations [127]. Using the United States Food and Drug Administration (FDA)-approved drugs, such as paclitaxel and doxorubicin, the platform demonstrated high potential for rapid and precise drug screening.

Beyond mechanical probes for drug screening, RE electrodes are also employed for concurrent physiological monitoring. Abbott et al. [128] developed a scalable microelectrode array enabling massively parallel electroporation and

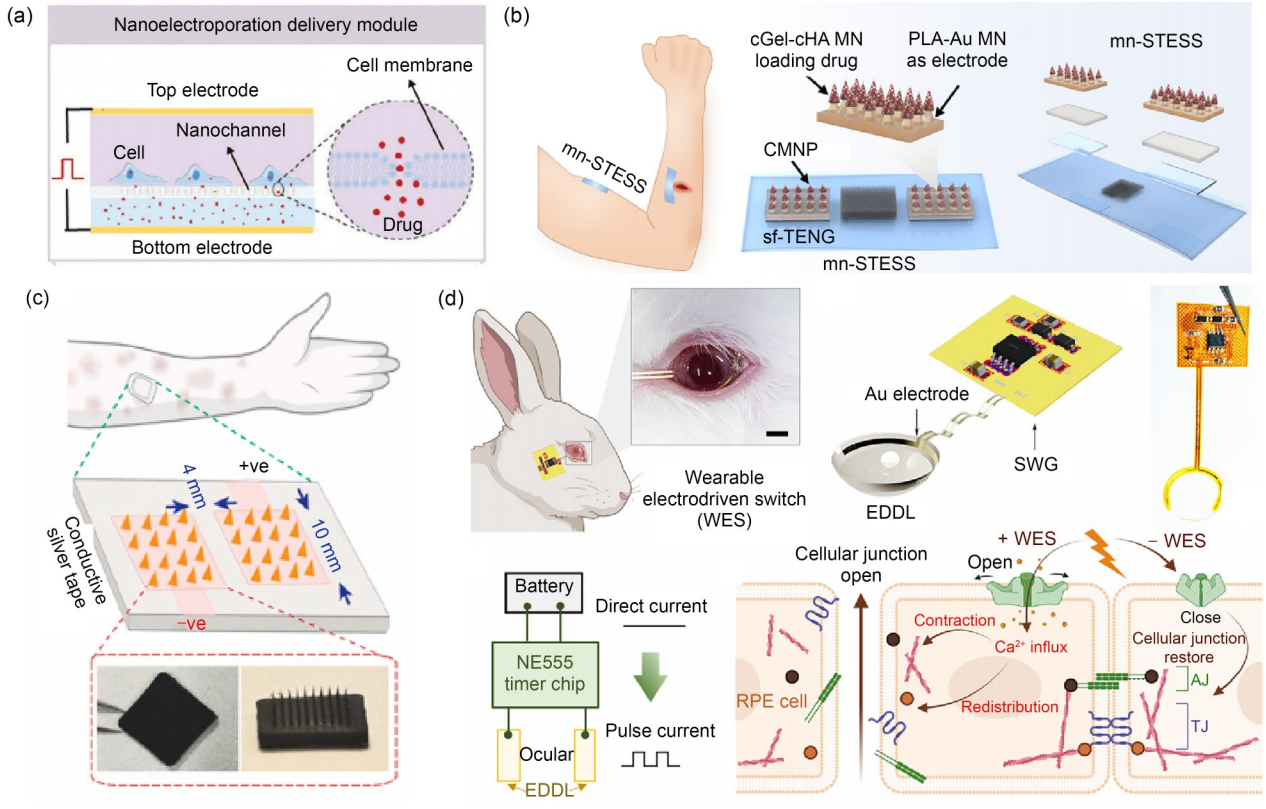


**Fig. 6** Application of RE in drug delivery. (a) Nanoelectroporation chip enabling rapid, efficient, and safe delivery of charged drug molecules (reproduced from [126], with permission from Wiley-VCH GmbH). (b) Microneedle-based self-powered transcutaneous electrical stimulation system (mn-STESS) improving epidermal growth factor pharmacodynamics in wound healing (reproduced from [132], licensed under CC BY 4.0). (c) Conductive microneedle patch for targeted delivery of antibacterial therapeutics into deep skin tissue (reproduced from [133], with permission from Elsevier Ltd.). (d) WES for noninvasive delivery of macromolecular drugs to the posterior eye (reproduced from [134], licensed under CC BY-NC-ND)

intracellular recording from thousands of cells. Vertically aligned nanocolumns permit long-term recording of extracellular and intracellular action potentials in cardiomyocytes and detect subtle changes in ion channel-specific drug responses [129]. Subsequent refinement by Wang et al. [130] introduced nanoporous electrodes that improved biosafety and enhanced electrode–cell coupling. The average intracellular coupling rate of the complementary metal-oxide semiconductor (CMOS) microhole array can reach 90%, more than twice that of the earlier design. These advances not only highlight the expanding utility of RE in electrophysiological studies but also suggest that similar array-based platforms could be adapted for high-throughput, cell-resolved molecular delivery. This approach represents a promising direction for scaling drug screening and development workflows.

Beyond in vitro drug evaluation, RE enables localized in vivo delivery that increases drug concentration at target sites while reducing systemic toxicity [131]. Among available systems, RE-integrated microneedles are widely used for drug delivery owing to their minimally invasive operation, ease of use, reduced dosing frequency, and strong biocompatibility. Yang et al. [132] designed a microneedle-based self-powered transcutaneous electrical stimulation system (mn-STESS) to enhance epidermal growth factor pharmacodynamics in wound healing (Fig. 6b). The system integrates a sliding freestanding TENG with a two-stage composite microneedle patch made from gold-coated polylactic acid/crosslinked gelatin and hyaluronic acid. The resulting mn-STESS markedly improved epidermal growth factor performance in vivo. Ghosh et al. [133] developed a conductive microneedle patch for targeted delivery of antibacterial agents into deep skin layers (Fig. 6c). These microneedles, fabricated from carbon nanotubes and gelatin methacrylate, enable electrically stimulated directional transport of small molecules into deep tissue layers. Notably, in vitro evaluation demonstrated that electrostimulated miconazole nitrate-loaded microneedles (M-MNs) exhibited superior biofilm penetration and fungicidal efficacy compared with either miconazole cream or nonelectrostimulated M-MNs. Nonetheless, microneedle-based techniques face challenges related to tissue trauma caused by needle penetration.

For noninvasive drug delivery, Qin et al. [134] developed a wearable electrodriven switch (WES) to noninvasively deliver macromolecular drugs to the posterior segment of the

eye (Fig. 6d). Integrating an electro-driven lens with a square-wave generator, the WES enhances drug penetration through the sclera–choroid–retina pathway via electrical stimulation. The system achieved 14% delivery efficiency for immunoglobulin G, approaching the 16% efficiency achieved through intravitreal injection, and substantially improved anti-vascular endothelial growth factor (anti-VEGF) therapy (showing 86% efficacy in choroidal neovascularization suppression) and anti-PD-L1 treatment (enhancing inhibition of choroidal melanoma growth compared with intravenous administration) without observable ocular toxicity.

## 4.4 Cellular sampling

Under the electric field of RE, the permeabilized membrane permits not only intracellular delivery but also the extraction of endogenous components. These retrieved materials enable multi-omic profiling through integration with gene sequencing or mass spectrometry, offering advantages over traditional intracellular analysis, which faces interference from complex cellular environments and finite fluorescent channel availability [135, 136].

The RE-coupled nanopipette single-cell sampling technique is widely used for extracting intracellular components from living cells. This approach relies on the manipulation of hollow microneedles under a microscope. First, a localized electric field is generated at the pipette tip to induce poration, followed by the application of negative pressure to withdraw cellular contents for downstream protein or genetic analysis. However, because only trace amounts are collected from each cell, sample loss during transfer and loading is common. To mitigate this, Li et al. [137] developed a method in which single cells migrate directly to the capillary tip via electro-driven transport, after which electroporation releases intracellular molecules for immediate mass spectrometry analysis (Fig. 7a). This method supports long-term metabolite

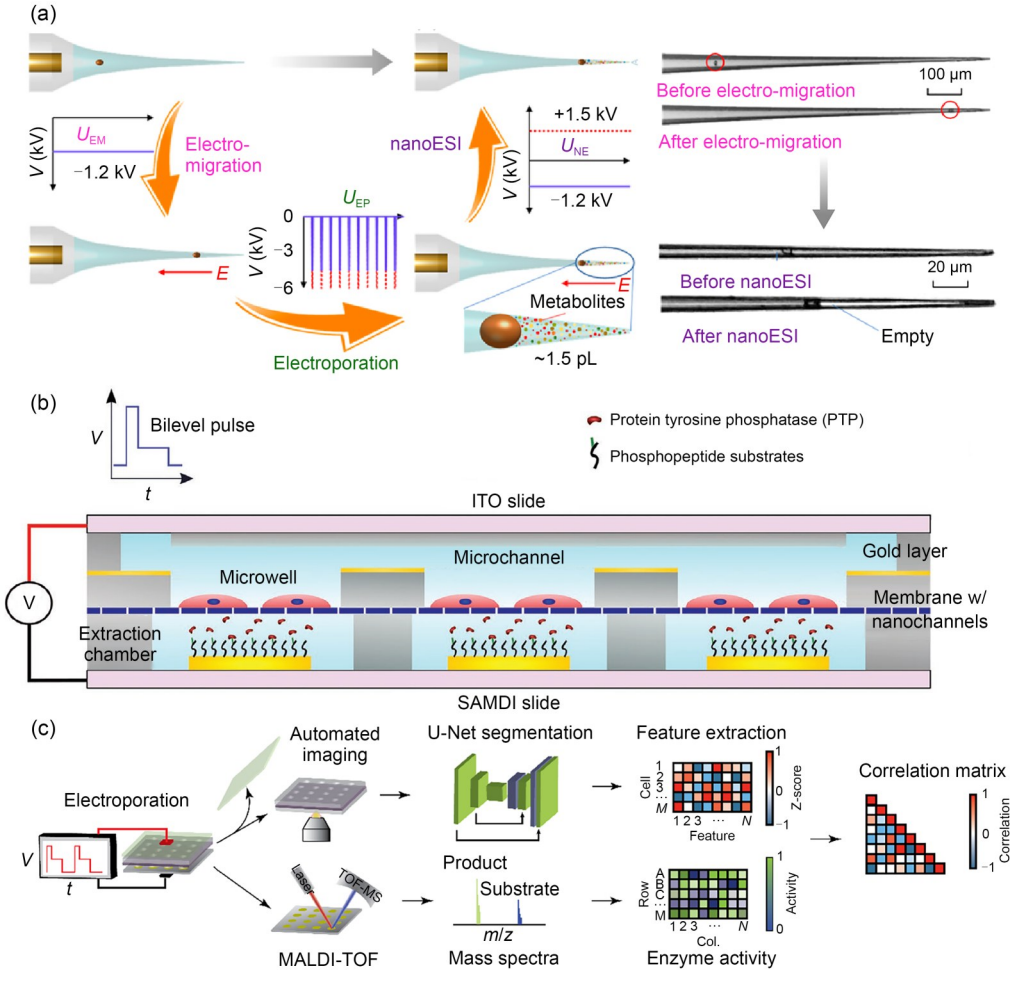


**Fig. 7** Cellular sampling using RE-based systems. (a) Single-cell electroporation for mass spectrometry analysis (reproduced from [137], with permission from the American Chemical Society). (b) On-chip sampling and analysis of living cells via SAMDI mass spectrometry (reproduced from [138], with permission from WILEY-VCH Verlag GmbH & Co. KGaA, Weinheim). (c) Deep learning-enhanced cell sampling for analysis of cell behavior and molecular profiles (reproduced from [139], with permission from the American Chemical Society). SAMDI: self-assembled monolayers for matrix-assisted laser desorption/ionization

monitoring in individual cells. Nevertheless, single-cell workflows still require substantial effort to generate statistically meaningful datasets.

To improve throughput, cell chips have been integrated with RE systems for large-scale sampling. Mukherjee et al. [138] created a microfluidic chip with microwell arrays enabling localized electroporation of cells (Fig. 7b). These RE-integrated platforms can process >10 000 cells in parallel while maintaining cell viability. Extracted enzymes were captured on self-assembled monolayers for matrix-assisted laser desorption/ionization (SAMDI) slides, allowing measurement of phosphatase activity and its oxidative response to $H_2O_2$ in live cells, demonstrating the system's suitability for long-term cell profiling. By combining deep learning-driven morphometric analysis with mass spectrometry-based protein activity mapping, this platform also establishes strong correlations between cellular behavior and molecular signatures (Fig. 7c) [139]. This integration highlights a promising direction for intelligent RE-enabled cell analyses.

Although RE is widely used for single-use sampling, extending it to repeated or longitudinal operation remains technically challenging. Major obstacles include electrode fouling, impedance drift, gas formation, and local pH changes, all of which affect cell viability and treatment consistency over time [140, 141]. To address these issues, several promising design strategies have been proposed: (1) using inert, high-capacity electrode materials (e.g., platinum and gold) [142]; (2) applying charge-balanced biphasic or symmetric waveforms to reduce Faradaic reactions and ion deposition [143]; (3) integrating real-time impedance or pH monitoring with closed-loop pulse control [144]; (4) incorporating microfluidic perfusion or biocompatible hydrogels to rapidly clear electrochemical byproducts [145]. Additionally, transferring the collected sample and replacing the electrode before each use remains standard practice [146]. Such approaches may help preserve electroporation stability and biocompatibility across multiple sessions, broadening the applicability of RE for dynamic cell monitoring.

## 5 Future directions and outlook

As a controllable method for cell membrane perforation and molecular transfer, RE has advanced rapidly through micro- and nano-fabrication innovations. With the emergence of flexible electronics, RE is evolving into a multifunctional in vivo biointerface capable of delivering biomolecules with spatiotemporal precision and extracting intracellular components for dynamic molecular profiling. This evolution is broadening RE from basic delivery toward applications in molecular mechanism analysis and personalized medicine.

For molecular mechanism profiling, RE is emerging as a key technology for single-cell and high-throughput studies, supporting efforts to decode cellular heterogeneity in molecular and behavioral phenotypes. Its compatibility with supramolecular constructs (e.g., CRISPR plasmids) and combinations of genetic regulators (e.g., mRNA cocktails) makes RE an appealing, nonviral, tunable approach for genome and transcriptome modulation across sensitive cell types, such as stem cells, neurons, and immune cells. In parallel, coupling RE with multi-omics technologies will enable minimally disruptive extraction of intracellular components, providing single-cell insights into gene expression, protein activity, and metabolic state.

For personalized precision medicine, next-generation RE systems are expected to achieve greater precision, lower operational voltages, and enhanced biocompatibility through minimally invasive and implantable devices. These systems will advance precision diagnostics and support the development of real-time, closed-loop therapies. Intelligent platforms with automated feedback control will enable adaptive, patient-specific operation for diagnostic and therapeutic applications. Flexible and biodegradable electrode materials, including soft electronics and resorbable thin films, will further enhance safety for in vivo uses, such as localized gene therapy, wound repair, and continuous biosensing in physiological settings.

In summary, the future of RE lies at the intersection of nanotechnology, systems biology, and translational medicine. By allowing controlled access to the intracellular space, RE can play an increasingly important role in fundamental biological research and the evolution of personalized healthcare.

**Acknowledgements** This work was supported by the following fundings: the National Key R&D Program of China (Nos. 2023YFC2415900, 2022YFB3205601, and 2022YFB3205602), Shandong Provincial Natural Science Foundation (Nos. ZR2024QB014 and ZR2024QF010), the National Natural Science Foundation of China (Nos. 22304006, T25B2018, 62471021, and T24B2006), the National Science Fund for Distinguished Young Scholars (No. T2425021), and the Fundamental Research Funds for the Central Universities (Nos. JKF-2025082276817 and JKF-20240574).

**Author contributions** Administrative support: YHZ and LQC; conceptualization: ZHZ; provision of study materials: FL and ZZD; collection and assembly of data: ZZD and YW; data analysis and interpretation: YHZ and ZHZ; manuscript writing: all authors; final approval of the manuscript: all authors.

## Declarations

**Conflict of interest** The authors declare that they have no conflict of interest.

**Ethical approval** This study does not contain any studies with human or animal subjects performed by any of the authors.

**Use of generative AI tools** No generative AI tools were used in the preparation of this manuscript.

## References


1. Yeagle PL (1989) Lipid regulation of cell membrane structure and function. *FASEB J* 3(7):1833–1842. https://doi.org/10.1096/fasebj.3.7.2469614
2. Suwalsky M (2015) Phospholipid bilayers. In: Mishra M (Ed.), Encyclopedia of Biomedical Polymers and Polymeric Biomaterials (1st Ed.). CRC Press, Boca Raton, p.6. https://www.taylorfrancis.com/chapters/edit/10.1081/E-EBPP-120051908/phospholipid-bilayers-mario-suwalsky [Accessed on 11 April 2026]
3. Lis LJ, McAlister M, Fuller N et al (1982) Interactions between neutral phospholipid bilayer membranes. *Biophys J* 37(3):657–665. https://doi.org/10.1016/S0006-3495(21)00385-4
4. Chen SA, Sun S, Moonen D et al (2019) CRISPR-READI: efficient generation of knockin mice by CRISPR RNP electroporation and AAV donor infection. *Cell Rep* 27(13):3780–3789. https://doi.org/10.1016/j.celrep.2019.05.103
5. Chen SA, Lee B, Lee AY et al (2016) Highly efficient mouse genome editing by CRISPR ribonucleoprotein electroporation of zygotes. *J Biol Chem* 291(28):14457–14467. https://doi.org/10.1074/jbc.M116.733154
6. Miao DQ, Giassetti MI, Ciccarelli M et al (2019) Simplified pipelines for genetic engineering of mammalian embryos by CRISPR-Cas9 electroporation. *Biol Reprod* 101(1):177–187. https://doi.org/10.1093/biolre/ioz075
7. Qiu XY, Sun YK, Gao JQ et al (2025) Progress and application of cell membrane engineering in living cell therapy. *Biomater Sci* 13(14):3733–3754. https://doi.org/10.1039/d5bm00120j
8. Wang LY, Zhu XY, Xu CY et al (2024) Artificial breakthrough of cell membrane barrier for transmembrane substance exchange: a review of recent progress. *Adv Funct Mater* 34(13):2311920. https://doi.org/10.1002/adfm.202311920
9. Reis R, Moraes I (2019) Structural biology and structure-function relationships of membrane proteins. *Biochem Soc Trans* 47(1):47–61. https://doi.org/10.1042/BST20180269
10. Kulbacka J, Choromańska A, Rossowska J et al (2017) Cell membrane transport mechanisms: ion channels and electrical properties of cell membranes. *Adv Anat Embryol Cell Biol* 227:39–58. https://doi.org/10.1007/978-3-319-56895-9_3
11. Tsong TY (1991) Electroporation of cell membranes. *Biophys J* 60(2):297–306. https://doi.org/10.1016/S0006-3495(91)82054-9
12. Graybill PM, Davalos RV (2020) Cytoskeletal disruption after electroporation and its significance to pulsed electric field therapies. *Cancers* 12(5):1132. https://doi.org/10.3390/cancers12051132
13. Aguilar AA, Ho MC, Chang E et al (2021) Permeabilizing cell membranes with electric fields. *Cancers* 13(9):2283. https://doi.org/10.3390/cancers13092283
14. Neumann E, Schaefer-Ridder M, Wang Y et al (1982) Gene transfer into mouse lyoma cells by electroporation in high electric fields. *EMBO J* 1(7):841–845. https://doi.org/10.1002/j.1460-2075.1982.tb01257.x
15. Liu XY, Wang H, Zhao ZL et al (2024) Advances in irreversible electroporation for prostate cancer. *Discov Oncol* 15(1):713. https://doi.org/10.1007/s12672-024-01570-4
16. Campelo SN, Huang PH, Buie CR et al (2023) Recent advancements in electroporation technologies: from bench to clinic. *Annu Rev Biomed Eng* 25:77–100. https://doi.org/10.1146/annurev-bioeng-110220-023800
17. Aghdasi M, Nazari M, Yonesi S (2023) A novel micro-device for simultaneous separation-trapping and double-trapping of particles by using dielectrophoresis: numerical and experimental study. *J Micromech Microeng* 33(10):105015. https://doi.org/10.1088/1361-6439/acef32
18. He S, Singh D, Helfield B (2022) An overview of cell membrane perforation and resealing mechanisms for localized drug delivery. *Pharmaceutics* 14(4):886. https://doi.org/10.3390/pharmaceutics14040886
19. Yao CG, Lv YP, Zhao YJ et al (2017) Synergistic combinations of short high-voltage pulses and long low-voltage pulses enhance irreversible electroporation efficacy. *Sci Rep* 7:15123. https://doi.org/10.1038/s41598-017-15494-3
20. Miklavcic D, Davalos RV (2015) Electrochemotherapy (ECT) and irreversible electroporation (IRE)-advanced techniques for treating deep-seated tumors based on electroporation. *Biomed Eng Online* 14(Suppl 3):I1. https://doi.org/10.1186/1475-925X-14-S3-I1
21. Weaver JC, Smith KC, Esser AT et al (2012) A brief overview of electroporation pulse strength-duration space: a region where additional intracellular effects are expected. *Bioelectrochemistry* 87:236–243. https://doi.org/10.1016/j.bioelechem.2012.02.007
22. Kandušer M, Miklavčič D, Pavlin M (2009) Mechanisms involved in gene electrotransfer using high- and low-voltage pulses: an in vitro study. *Bioelectrochemistry* 74(2):265–271. https://doi.org/10.1016/j.bioelechem.2008.09.002
23. Tieleman DP (2004) The molecular basis of electroporation. *BMC Biochem* 5:10. https://doi.org/10.1186/1471-2091-5-10
24. Melikov KC, Frolov VA, Shcherbakov A et al (2001) Voltage-induced nonconductive pre-pores and metastable single pores in unmodified planar lipid bilayer. *Biophys J* 80(4):1829–1836. https://doi.org/10.1016/S0006-3495(01)76153-X
25. Gianulis EC, Lee JM, Jiang CQ et al (2015) Electroporation of mammalian cells by nanosecond electric field oscillations and its inhibition by the electric field reversal. *Sci Rep* 5:13818. https://doi.org/10.1038/srep13818
26. Beebe SJ, White J, Blackmore P et al (2004) Nanosecond pulsed electric fields mimic natural cell signal transduction mechanisms. In: 26th International Power Modulator Symposium and High-Voltage Workshop, p.220–223. https://doi.org/10.1109/MODSYM.2004.1433548
27. Posadas O (2022) Electroporation Optimization. Master's Dissertation, Lehigh University, USA. https://preserve.lehigh.edu/lehigh-scholarship/graduate-publications-theses-dissertations/theses-dissertations/electroporation [Accessed on 11 April 2026]
28. Krassowska W, Filev PD (2007) Modeling electroporation in a single cell. *Biophys J* 92(2):404–417. https://doi.org/10.1529/biophysj.106.094235
29. Bennett WFD, Tieleman DP (2011) Water defect and pore formation in atomistic and coarse-grained lipid membranes: pushing the limits of coarse graining. *J Chem Theory Comput* 7(9):2981–2988. https://doi.org/10.1021/ct200291v
30. Marracino P, Caramazza L, Montagna M et al (2022) Electric-driven membrane poration: a rationale for water role in the kinetics of pore formation. *Bioelectrochemistry* 143:107987. https://doi.org/10.1016/j.bioelechem.2021.107987
31. Weaver JC, Chizmadzhev YA (1996) Theory of electroporation: a review. *Bioelectrochem Bioenerg* 41(2):135–160. https://doi.org/10.1016/S0302-4598(96)05062-3
32. DeBruin KA, Krassowska W (1999) Modeling electroporation in a single cell. I. Effects of field strength and rest potential.

*Biophys J* 77(3):1213–1224. https://doi.org/10.1016/S0006-3495(99)76973-0
33. Ruzgys P, Jakutavičiūtė M, Šatkauskienė I et al (2019) Effect of electroporation medium conductivity on exogenous molecule transfer to cells in vitro. *Sci Rep* 9(1):1436. https://doi.org/10.1038/s41598-018-38287-8
34. Joshi RP, Schoenbach KH (2000) Electroporation dynamics in biological cells subjected to ultrafast electrical pulses: a numerical simulation study. *Phys Rev E* 62(1):1025–1033. https://doi.org/10.1103/physreve.62.1025
35. Vasilkoski Z, Esser AT, Gowrishankar TR et al (2006) Membrane electroporation: the absolute rate equation and nanosecond time scale pore creation. *Phys Rev E* 74:021904. https://doi.org/10.1103/PhysRevE.74.021904
36. Bubnis G, Grubmüller H (2020) Sequential water and headgroup merger: membrane poration paths and energetics from MD simulations. *Biophys J* 119(12):2418–2430. https://doi.org/10.1016/j.bpj.2020.10.037
37. Zheng W, Mi Y, Ma C et al (2023) A perspective on modeling pore energy and pulsed electromagnetic field induced cell membrane perforation. *J Appl Phys* 133(12):120901. https://doi.org/10.1063/5.0139065
38. Aycock KN, Davalos RV (2019) Irreversible electroporation: background, theory, and review of recent developments in clinical oncology. *Bioelectricity* 1(4):214–234. https://doi.org/10.1089/bioe.2019.0029
39. Ding LJ, Fang Z, Moser MAJ et al (2023) A single-cell electroporation model for quantitatively estimating the pore area ratio by high-frequency irreversible electroporation. *Appl Sci* 13(3):1808. https://doi.org/10.3390/app13031808
40. Liu HT, Tao XN, Xiang XW et al (2024) Modeling of cell electroporation with emphasis on ions transport-induced dynamic alterations in membrane conductivity. *IEEE Trans Dielectr Electr Insul* 31(2):852–860. https://doi.org/10.1109/TDEI.2023.3327218
41. Li JB, Lin H (2011) Numerical simulation of molecular uptake via electroporation. *Bioelectrochemistry* 82(1):10–21. https://doi.org/10.1016/j.bioelechem.2011.04.006
42. Neumann E, Toensing K, Kakorin S et al (1998) Mechanism of electroporative dye uptake by mouse B cells. *Biophys J* 74(1): 98–108. https://doi.org/10.1016/S0006-3495(98)77771-9
43. Ringel-Scaia VM, Beitel-White N, Lorenzo MF et al (2019) High-frequency irreversible electroporation is an effective tumor ablation strategy that induces immunologic cell death and promotes systemic anti-tumor immunity. *eBioMedicine* 44:112–125. https://doi.org/10.1016/j.ebiom.2019.05.036
44. Geboers B, Scheffer HJ, Graybill PM et al (2020) High-voltage electrical pulses in oncology: irreversible electroporation, electrochemotherapy, gene electrotransfer, electrofusion, and electroimmunotherapy. *Radiology* 295(2):254–272. https://doi.org/10.1148/radiol.2020192190
45. Tam C, Idone V, Devlin C et al (2010) Exocytosis of acid sphingomyelinase by wounded cells promotes endocytosis and plasma membrane repair. *J Cell Biol* 189(6):1027–1038. https://doi.org/10.1083/jcb.201003053
46. Castro-Gomes T, Corrotte M, Tam C et al (2016) Plasma membrane repair is regulated extracellularly by proteases released from lysosomes. *PLoS ONE* 11(3):e0152583. https://doi.org/10.1371/journal.pone.0152583
47. Batista Napotnik T, Polajžer T, Miklavčič D (2021) Cell death due to electroporation – a review. *Bioelectrochemistry* 141:107871. https://doi.org/10.1016/j.bioelechem.2021.107871
48. Mirshahi S, Vahedi B, Aryana K et al (2024) Cancerous cell viability affected by synergism between electric pulses and a low dose of silver nanoparticle: an adaptive neuro-fuzzy inference system. *Med Nov Technol Devices* 21:100280. https://doi.org/10.1016/j.medntd.2023.100280
49. Schwan HP (1957) Electrical properties of tissue and cell suspensions. In: Advances in Biological and Medical Physics (1st Ed.). *Elsevier*, p.147–209. https://doi.org/10.1016/b978-1-4832-3111-2.50008-0
50. Kotnik T, Rems L, Tarek M et al (2019) Membrane electroporation and electropermeabilization: mechanisms and models. *Annu Rev Biophys* 48:63–91. https://doi.org/10.1146/annurev-biophys-052118-115451
51. Gürsoy G, Esmekaya MA, Çiçek Z (2025) The effects of microseconds electroporation on pore size, viability and mitochondrial membrane potential of cervical cancer cells. *Bezmialem Sci* 13(1): 58–64. https://doi.org/10.14235/bas.galenos.2024.40374
52. Brooks JR, Heiman TC, Lorenzen SR et al (2023) Transepithelial electrical impedance increase following porous substrate electroporation enables label-free delivery. bioRxiv. https://doi.org/10.1101/2023.10.17.562630
53. Rols MP, Teissié J (1998) Electropermeabilization of mammalian cells to macromolecules: control by pulse duration. *Biophys J* 75(3):1415–1423. https://doi.org/10.1016/S0006-3495(98)74060-3
54. Choi SE, Khoo H, Hur SC (2022) Recent advances in microscale electroporation. *Chem Rev* 122(13):11247–11286. https://doi.org/10.1021/acs.chemrev.1c00677
55. Lee WG, Demirci U, Khademhosseini A (2009) Microscale electroporation: challenges and perspectives for clinical applications. *Integr Biol* 1(3):242–251. https://doi.org/10.1039/b819201d
56. Saulis G, Saulė R (2012) Size of the pores created by an electric pulse: microsecond vs millisecond pulses. *Biochim Biophys Acta BBA Biomembr* 1818(12):3032–3039. https://doi.org/10.1016/j.bbamem.2012.06.018
57. Pavlin M, Kandušer M (2015) New insights into the mechanisms of gene electrotransfer: experimental and theoretical analysis. *Sci Rep* 5:9132. https://doi.org/10.1038/srep09132
58. Sokołowska E, Błachnio-Zabielska AU (2019) A critical review of electroporation as a plasmid delivery system in mouse skeletal muscle. *Int J Mol Sci* 20(11):2776. https://doi.org/10.3390/ijms20112776
59. Mickevičiūtė E, Radzevičiūtė-Valčiukė E, Malyško-Ptašinskė V et al (2024) The effects of bipolar cancellation phenomenon on nano-electrochemotherapy of melanoma tumors: in vitro and in vivo pilot. *Int J Mol Sci* 25(17):9338. https://doi.org/10.3390/ijms25179338
60. Kandušer M, Šentjurc M, Miklavčič D (2008) The temperature effect during pulse application on cell membrane fluidity and permeabilization. *Bioelectrochemistry* 74(1):52–57. https://doi.org/10.1016/j.bioelechem.2008.04.012
61. Muratori C, Pakhomov AG, Gianulis EC et al (2016) The cytotoxic synergy of nanosecond electric pulses and low temperature leads to apoptosis. *Sci Rep* 6:36835. https://doi.org/10.1038/srep36835
62. Müller WA, Sarkis JR, Marczak LDF et al (2022) Molecular dynamics insights on temperature and pressure effects on electroporation. *Biochim Biophys Acta BBA Biomembr* 1864(12):184049. https://doi.org/10.1016/j.bbamem.2022.184049
63. Kotnik T, Pucihar G, Miklavcic D (2010) Induced transmembrane voltage and its correlation with electroporation-mediated molecular transport. *J Membr Biol* 236(1):3–13. https://doi.org/10.1007/s00232-010-9279-9
64. Al-Sakere B, Bernat C, Andre F et al (2007) A study of the

immunological response to tumor ablation with irreversible electroporation. *Technol Cancer Res Treat* 6(4):301–306. https://doi.org/10.1177/153303460700600406
65. Marcellier G, Le Berre T, Rivallin P et al (2025) Electroporation for the treatment of pancreatic ductal adenocarcinoma: a systematic review of preclinical and clinical studies. *Clin Transl Gastroenterol* 16(11):e00911. https://doi.org/10.14309/ctg.0000000000000911
66. Sano MB, Fan RE, Xing L (2017) Asymmetric waveforms decrease lethal thresholds in high frequency irreversible electroporation therapies. *Sci Rep* 7:40747. https://doi.org/10.1038/srep40747
67. Jacobs EJ, Santos PP, Davalos RV (2025) Effects of interphase and interpulse delays on tissue impedance and pulsed field ablation. *Ann Biomed Eng* 53(8):1962–1974. https://doi.org/10.1007/s10439-025-03757-4
68. Miklavčič D, Mali B, Kos B et al (2014) Electrochemotherapy: from the drawing board into medical practice. *Biomed Eng Online* 13(1):29. https://doi.org/10.1186/1475-925X-13-29
69. Lindelauf KHK, Baragona M, Baumann M et al (2023) Pulse parameters and thresholds for (ir)reversible electroporation on hepatocellular carcinoma cells in vitro. *Technol Cancer Res Treat* 22:1–8. https://doi.org/10.1177/15330338221136694
70. Chen YS, Huang CH, Pai PC et al (2023) A review on microfluidics-based impedance biosensors. *Biosensors* 13(1):83. https://doi.org/10.3390/bios13010083
71. Dong SY, Liu X, Bi Y et al (2023) Adaptive design of mRNA-loaded extracellular vesicles for targeted immunotherapy of cancer. *Nat Commun* 14:6610. https://doi.org/10.1038/s41467-023-42365-5
72. Liu F, Yang Z, Yao R et al (2022) Bulk electroporation for intracellular delivery directly driven by mechanical stimulus. *ACS Nano* 16(11):19363–19372. https://doi.org/10.1021/acsnano.2c08945
73. Huang PH, Chen SJ, Shiver AL et al (2022) M-TUBE enables large-volume bacterial gene delivery using a high-throughput microfluidic electroporation platform. *PLoS Biol* 20(9):e3001727. https://doi.org/10.1371/journal.pbio.3001727
74. Ma YF, Sun LL, Zhang JJ et al (2023) Exosomal mRNAs for angiogenic–osteogenic coupled bone repair. *Adv Sci* 10(33): 2302622. https://doi.org/10.1002/advs.202302622
75. Dong ZZ, Jiao YL, Xie BT et al (2020) On-chip multiplexed single-cell patterning and controllable intracellular delivery. *Microsyst Nanoeng* 6:2. https://doi.org/10.1038/s41378-019-0112-z
76. Gallego-Perez D, Otero JJ, Czeisler C et al (2016) Deterministic transfection drives efficient nonviral reprogramming and uncovers reprogramming barriers. *Nanomed Nanotechnol Biol Med* 12(2): 399–409. https://doi.org/10.1016/j.nano.2015.11.015
77. Pathak N, Patino CA, Ramani N et al (2023) Cellular delivery of large functional proteins and protein-nucleic acid constructs via localized electroporation. *Nano Lett* 23(8):3653–3660. https://doi.org/10.1021/acs.nanolett.2c04374
78. Kang W, Giraldo-Vela JP, Nathamgari SSP et al (2014) Microfluidic device for stem cell differentiation and localized electroporation of postmitotic neurons. *Lab Chip* 14(23):4486–4495. https://doi.org/10.1039/c4lc00721b
79. Schmiderer L, Subramaniam A, Žemaitis K et al (2020) Efficient and nontoxic biomolecule delivery to primary human hematopoietic stem cells using nanostraws. *Proc Natl Acad Sci USA* 117(35): 21267–21273. https://doi.org/10.1073/pnas.2001367117
80. Shokouhi AR, Chen YP, Yoh HZ et al (2023) Electroactive nanoinjection platform for intracellular delivery and gene silencing. *J Nanobiotechnol* 21(1):273. https://doi.org/10.1186/s12951-023-02056-1
81. Yan KS, Todo H, Sugibayashi K (2010) Transdermal drug delivery by in-skin electroporation using a microneedle array. *Int J Pharm* 397(1–2):77–83. https://doi.org/10.1016/j.ijpharm.2010.06.052
82. Wang Y, Qu J, Xiong CX et al (2024) Transdermal microarrayed electroporation for enhanced cancer immunotherapy based on DNA vaccination. *Proc Natl Acad Sci USA* 121(25):e2322264121. https://doi.org/10.1073/pnas.2322264121
83. Punjiya M, Nejad HR, Mathews J et al (2019) A flow through device for simultaneous dielectrophoretic cell trapping and AC electroporation. *Sci Rep* 9(1):11988. https://doi.org/10.1038/s41598-019-48198-x
84. Dong RH, Liu XY, Cheng SY et al (2021) Highly stretchable metal-polymer conductor electrode array for electrophysiology. *Adv Healthc Mater* 10(4):e2000641. https://doi.org/10.1002/adhm.202000641
85. Šmerc R, Miklavčič D, Mahnič-Kalamiza S (2025) An experimentally validated numerical model of pH changes in surrogate tissue induced by electroporation pulses. *Electrochim Acta* 511: 145363. https://doi.org/10.1016/j.electacta.2024.145363
86. Chung T, Wang JQ, Wang J et al (2015) Electrode modifications to lower electrode impedance and improve neural signal recording sensitivity. *J Neural Eng* 12(5):056018. https://doi.org/10.1088/1741-2560/12/5/056018
87. Tay A, Melosh N (2019) Nanostructured materials for intracellular cargo delivery. *Acc Chem Res* 52(9):2462–2471. https://doi.org/10.1021/acs.accounts.9b00272
88. Gharia AA, Bradfield CJ, Jenkins EPW et al (2024) Efficient electroporation in primary cells with PEDOT:PSS electrodes. *Sci Adv* 10(43):eado5042. https://doi.org/10.1126/sciadv.ado5042
89. Xie YB, Wang Y, Du HX (2013) Electrochemical capacitance performance of titanium nitride nanoarray. *Mater Sci Eng B* 178(20): 1443–1451. https://doi.org/10.1016/j.mseb.2013.09.005
90. Lin ZC, Xie C, Osakada Y et al (2014) Iridium oxide nanotube electrodes for sensitive and prolonged intracellular measurement of action potentials. *Nat Commun* 5:3206. https://doi.org/10.1038/ncomms4206
91. Ren N, Hang C, Liu XY et al (2022) Printable metal–polymer conductors for local drug delivery. *Nano Lett* 22(18):7554–7562. https://doi.org/10.1021/acs.nanolett.2c02548
92. Ouyang MX, Hill W, Lee JH et al (2017) Microscale symmetrical electroporator array as a versatile molecular delivery system. *Sci Rep* 7:44757. https://doi.org/10.1038/srep44757
93. Huang H, Wei ZW, Huang YY et al (2011) An efficient and high-throughput electroporation microchip applicable for siRNA delivery. *Lab Chip* 11(1):163–172. https://doi.org/10.1039/c0lc00195c
94. Iwai K, Wehrs M, Garber M et al (2022) Scalable and automated CRISPR-based strain engineering using droplet microfluidics. *Microsyst Nanoeng* 8:31. https://doi.org/10.1038/s41378-022-00357-3
95. Kauth A, Mildner AK, Hegel L et al (2024) Development of specialized microelectrode arrays with local electroporation functionality. *Ann Biomed Eng* 52(1):12–21. https://doi.org/10.1007/s10439-023-03268-0
96. Hang C, Ding L, Cheng SY et al (2021) A soft and absorbable temporary epicardial pacing wire. *Adv Mater* 33(36):2101447.

https://doi.org/10.1002/adma.202101447
97. Xu XK, Guo L, Liu H et al (2024) Stretchable electronic facial masks for skin electroporation. *Adv Funct Mater* 34(9):2311144. https://doi.org/10.1002/adfm.202311144
98. Cheng SY, Hang C, Ding L et al (2020) Electronic blood vessel. *Matter* 3(5):1664–1684. https://doi.org/10.1016/j.matt.2020.08.029
99. Wu H, Wang YQ, Li H et al (2024) Accelerated intestinal wound healing via dual electrostimulation from a soft and biodegradable electronic bandage. *Nat Electron* 7(4):299–312. https://doi.org/10.1038/s41928-024-01138-8
100. Muralidharan A, Pesch GR, Hubbe H et al (2022) Microtrap array on a chip for localized electroporation and electro-gene transfection. *Bioelectrochemistry* 147:108197. https://doi.org/10.1016/j.bioelechem.2022.108197
101. Jiang J, Liu J, Liu XM et al (2024) Coupling of nanostraws with diverse physicochemical perforation strategies for intracellular DNA delivery. *J Nanobiotechnol* 22(1):131. https://doi.org/10.1186/s12951-024-02392-w
102. Yin DD, Wang P, Hao YC et al (2025) A battery-free nanofluidic intracellular delivery patch for internal organs. *Nature* 642(8069): 1051–1061. https://doi.org/10.1038/s41586-025-08943-x
103. Tang FC, Barbacioru C, Wang YZ et al (2009) mRNA-Seq whole-transcriptome analysis of a single cell. *Nat Methods* 6(5):377–382. https://doi.org/10.1038/nmeth.1315
104. Vallabhajosula S (2023) Cell and molecular biology. In: Molecular Imaging and Targeted Therapy. Springer International Publishing, p.117–145. https://doi.org/10.1007/978-3-031-23205-3_7
105. Hastie ND, Bishop JO (1976) The expression of three abundance classes of messenger RNA in mouse tissues. *Cell* 9(4):761–774. https://doi.org/10.1016/0092-8674(76)90139-2
106. Stolwijk JA, Wegener J (2020) Impedance analysis of adherent cells after in situ electroporation-mediated delivery of bioactive proteins, DNA and nanoparticles in μL-volumes. *Sci Rep* 10(1): 21331. https://doi.org/10.1038/s41598-020-78096-6
107. van den Bos W, de Bruin DM, Muller BG et al (2014) The safety and efficacy of irreversible electroporation for the ablation of prostate cancer: a multicentre prospective human in vivo pilot study protocol. *BMJ Open* 4(10):e006382. https://doi.org/10.1136/bmjopen-2014-006382
108. Chang LQ, Wang YC, Ershad F et al (2019) Wearable devices for single-cell sensing and transfection. *Trends Biotechnol* 37(11): 1175–1188. https://doi.org/10.1016/j.tibtech.2019.04.001
109. Robin P, Gerber-Lemaire S (2022) Design and preparation of sensing surfaces for capacitive biodetection. *Biosensors* 13(1):17. https://doi.org/10.3390/bios13010017
110. Chang LQ, Howdyshell M, Liao WC et al (2015) Magnetic tweezers-based 3D microchannel electroporation for high-throughput gene transfection in living cells. *Small* 11(15):1818–1828. https://doi.org/10.1002/smll.201402564
111. Dong ZZ, Wang YS, Xu GL et al (2024) Genetic and phenotypic profiling of single living circulating tumor cells from patients with microfluidics. *Proc Natl Acad Sci USA* 121(19):e2315168121. https://doi.org/10.1073/pnas.2315168121
112. Dong ZZ, Yan S, Liu B et al (2021) Single living cell analysis nanoplatform for high-throughput interrogation of gene mutation and cellular behavior. *Nano Lett* 21(11):4878–4886. https://doi.org/10.1021/acs.nanolett.1c00199
113. Sun H, Dong ZZ, Zhang QY et al (2022) Companion-Probe & Race platform for interrogating nuclear protein and migration of living cells. *Biosens Bioelectron* 210:114281. https://doi.org/10.1016/j.bios.2022.114281
114. Wan FQ, Dong ZZ, Liu B et al (2022) Sensitive interrogation of enhancer activity in living cells on a nanoelectroporation-probing platform. *ACS Sens* 7(12):3671–3681. https://doi.org/10.1021/acssensors.2c01187
115. Snijder B, Pelkmans L (2011) Origins of regulated cell-to-cell variability. *Nat Rev Mol Cell Biol* 12(2):119–125. https://doi.org/10.1038/nrm3044
116. Santillo S, Schiano Moriello A, Di Maio V (2014) Electrophysiological variability in the SH-SY5Y cellular line. *Gen Physiol Biophys* 33(1):121–129. https://doi.org/10.4149/gpb_2013071
117. Yang RG, Lemaître V, Huang CJ et al (2018) Monoclonal cell line generation and CRISPR/Cas9 manipulation via single-cell electroporation. *Small* 14(12):e1702495. https://doi.org/10.1002/smll.201702495
118. Park SH, Kim Y, Kim M et al (2025) mRNA vaccine delivery via intramuscular electroporation induces protective antiviral immune responses in mice. *Appl Sci* 15(8):4428. https://doi.org/10.3390/app15084428
119. Wang JL, Lu YF, Zhang R et al (2024) Modulating and imaging macrophage reprogramming for cancer immunotherapy. *Phenomics* 4(4):401–414. https://doi.org/10.1007/s43657-023-00154-6
120. Guo KM, Lai YK, Han YR et al (2025) SIMPLE: a one-pot RPA-Cas12b method for single nucleotide variations identification with an expanded scope and clinical applications. *Phenomics* 5(4): 418–434. https://doi.org/10.1007/s43657-025-00240-x
121. Mendell JR, Al-Zaidy SA, Rodino-Klapac LR et al (2021) Current clinical applications of in vivo gene therapy with AAVs. *Mol Ther* 29(2):464–488. https://doi.org/10.1016/j.ymthe.2020.12.007
122. Athanasopoulos T, Munye MM, Yáñez-Muñoz RJ (2017) Nonintegrating gene therapy vectors. *Hematol Oncol Clin North Am* 31(5):753–770. https://doi.org/10.1016/j.hoc.2017.06.007
123. Tang R, Xu ZG (2020) Gene therapy: a double-edged sword with great powers. *Mol Cell Biochem* 474(1):73–81. https://doi.org/10.1007/s11010-020-03834-3
124. Liu F, Sun H, Liu B et al (2025) A nano-electro-platform enabling evolutionary screening and remodeling of tumor cells for metastasis inhibition. *Adv Sci* 12(34):e07684. https://doi.org/10.1002/advs.202507684
125. Gallego-Perez D, Pal D, Ghatak S et al (2017) Topical tissue nano-transfection mediates non-viral stroma reprogramming and rescue. *Nat Nanotechnol* 12(10):974–979. https://doi.org/10.1038/nnano.2017.134
126. Hang XX, Huang ZC, He SQ et al (2024) A nano-electroporation-DNA tensioner platform enhances intracellular delivery and mechanical analysis toward rapid drug assessment. *Small Methods* 8(3):e2300915. https://doi.org/10.1002/smtd.202300915
127. Li Y, Wang ZN, Ajani JA et al (2021) Drug resistance and cancer stem cells. *Cell Commun Signal* 19(1):19. https://doi.org/10.1186/s12964-020-00627-5
128. Abbott J, Ye TY, Krenek K et al (2020) A nanoelectrode array for obtaining intracellular recordings from thousands of connected neurons. *Nat Biomed Eng* 4(2):232–241. https://doi.org/10.1038/s41551-019-0455-7
129. Xie C, Lin ZL, Hanson L et al (2012) Intracellular recording of action potentials by nanopillar electroporation. *Nat Nanotechnol* 7(3):185–190. https://doi.org/10.1038/nnano.2012.8

130. Wang J, Jung WB, Gertner RS et al (2025) Synaptic connectivity mapping among thousands of neurons via parallelized intracellular recording with a microhole electrode array. *Nat Biomed Eng* 9(7):1144–1154. https://doi.org/10.1038/s41551-025-01352-5
131. Lian H, Liu Y, Wang H et al (2024) Preclinical testing of immunotoxicity for animal-derived dermal materials. *Med Nov Technol Devices* 23:100323. https://doi.org/10.1016/j.medntd.2024.100323
132. Yang Y, Luo RZ, Chao SY et al (2022) Improved pharmacodynamics of epidermal growth factor via microneedles-based self-powered transcutaneous electrical stimulation. *Nat Commun* 13(1): 6908. https://doi.org/10.1038/s41467-022-34716-5
133. Ghosh S, Zheng MJ, He JH et al (2025) Electrically-driven drug delivery into deep cutaneous tissue by conductive microneedles for fungal infection eradication and protective immunity. *Biomaterials* 314:122908. https://doi.org/10.1016/j.biomaterials.2024.122908
134. Qin X, Shi HL, Li HY et al (2025) Wearable electrodriven switch actively delivers macromolecular drugs to fundus in non-invasive and controllable manners. *Nat Commun* 16(1):33. https://doi.org/10.1038/s41467-024-55336-1
135. Shiomi A, Kaneko T, Nishikawa K et al (2024) High-throughput mechanical phenotyping and transcriptomics of single cells. *Nat Commun* 15(1):3812. https://doi.org/10.1038/s41467-024-48088-5
136. Péter B, Ausbüttel T, Kanyo N et al (2025) In situ monitoring of cell adhesion kinetics using label-free optical biosensors: evaluating anticancer potential and selectivity of natural compounds. View (early access). https://doi.org/10.1002/viw.20250061
137. Li ZS, Wang ZM, Pan JM et al (2020) Single-cell mass spectrometry analysis of metabolites facilitated by cell electro-migration and electroporation. *Anal Chem* 92(14):10138–10144. https://doi.org/10.1021/acs.analchem.0c02147
138. Mukherjee P, Berns EJ, Patino CA et al (2020) Temporal sampling of enzymes from live cells by localized electroporation and quantification of activity by SAMDI mass spectrometry. *Small* 16(26):e2000584. https://doi.org/10.1002/smll.202000584
139. Patino CA, Mukherjee P, Berns EJ et al (2022) High-throughput microfluidics platform for intracellular delivery and sampling of biomolecules from live cells. *ACS Nano* 16(5):7937–7946. https://doi.org/10.1021/acsnano.2c00698
140. Ungureanu C, Răileanu S, Ștefan DS et al (2025) Electric field effects on microbial cell properties: implications for detection and control in wastewater systems. *Environments* 12(10):343. https://doi.org/10.3390/environments12100343
141. Velizarov S (1999) Electric and magnetic fields in microbial biotechnology: possibilities, limitations, and perspectives. *Electro Magnetobiol* 18(2):185–212. https://doi.org/10.3109/15368379909012912
142. Raptis L, Balboa V, Hsu T et al (2003) In situ electroporation of large numbers of cells using minimal volumes of material. *Anal Biochem* 317(1):124–128. https://doi.org/10.1016/s0003-2697(03)00078-2
143. Aplin FP, Fridman GY (2019) Implantable direct current neural modulation: theory, feasibility, and efficacy. *Front Neurosci* 13: 379. https://doi.org/10.3389/fnins.2019.00379
144. Maglietti F, Michinski S, Olaiz N et al (2013) The role of pH fronts in tissue electroporation based treatments. *PLoS ONE* 8(11): e80167. https://doi.org/10.1371/journal.pone.0080167
145. Movahed S, Li DQ (2011) Microfluidics cell electroporation. *Microfluid Nanofluid* 10(4):703–734. https://doi.org/10.1007/s10404-010-0716-y
146. Huang ZC, Liu F, Zhi DY et al (2025) Nano-electro-sampling and intelligent analysis system for real-time gene profiling of living cells. *Small* 21(46):e06688. https://doi.org/10.1002/smll.202506688